Institut für Hydrologie
Albert – Ludwigs Universität Freiburg im Breisgau

Verweilzeitmodellierung mit ^{18}O auf der Grundlage eines konzeptuellen Niederschlags-Abfluss Modells

---

Transit time modelling with ^{18}O based on a conceptual precipitation-runoff model

René Capell

Diplomarbeit unter der Leitung von Prof. Dr. Christian Leibundgut

Freiburg im Breisgau, Februar 2007

Institut für Hydrologie
Albert – Ludwigs Universität Freiburg im Breisgau

Verweilzeitmodellierung mit ^{18}O auf der Grundlage eines konzeptuellen Niederschlags-Abfluss Modells

---

Transit time modelling with ^{18}O based on a conceptual precipitation-runoff model

Autor: René Capell

Referent: Prof. Dr. Ch. Leibundgut
Koreferent: Dr. J. Lange

Diplomarbeit unter der Leitung von Prof. Dr. Christian Leibundgut

Freiburg im Breisgau, Februar 2007

Contents

List of Figures

List of Tables

Danksagungen

Herrn Prof. Dr. Ch. Leibundgut danke ich für die Vergabe der Diplomarbeit und die Ermöglichung des Aufenthalts in Schweden im Rahmen dieser Diplomarbeit.

Ein herzlicher Dank geht an Herrn Dr. J. Lange für die sehr gute Betreuung und die vielen Diskussionen.

Ausserdem danke ich Herrn Dr. J. Seibert für das zur Verfügung stellen des HBV Codes, die Aufnahme und sehr gute Betreuung der Arbeit während meines Aufenthaltes in Stockholm, und ich möchte Herrn Dr. Ch. Külls danken für die vielen wertvollen Diskussionsbeiträge vor allem zu Beginn der Diplomarbeit.

Des weiteren danke ich summarisch meinen Mitdiplomanden und Büroteilern für die unzähligen hilfreichen Gespräche und allen Korrekturlesern fürs Korrekturlesen: Inga Capell, Timo Ehnes, Ingo Heidbüchel, Bredo Leipprand, Thorben Römer, Tobias Schütz, Stephan Tillmanns, Christian Wiesendanger, Julia Zábori.

Ein besonderer Dank noch mal an Stephan für die ganz hervorragende Zeit in Schweden!

Zu guter Letzt danke ich meinen Eltern, die mir dieses Studium letztendlich ermöglicht haben und meinen Schwestern für die generelle Unterstützung.

Summary

The objective of this thesis was firstly to develop a conceptual transit time model and integrate it into the framework of the HBV model and secondly apply the newly implemented model in two mesoscaled catchments in the Southern Black Forest in order to evaluate the long-term effects of the drought summer 2003.

Daily time series of precipitation, temperature, humidity, and runoff were available as well as weekly time series of δ^{18}O in precipitation and stream water for both catchments and the investigation period 2000 – 2006.

In a first step, the model concept was developed, it now includes a storage extention with the ability to store percolating water volumes alongside with a concentration and entry date, and an exponential-shaped adjustable distribution function, which allows to adjust the contribution scheme of the storage components according to their residence time in the storage. I.e. it is possible to amplify the runoff contribution of the younger storage components in a exponential-shaped scheme.

Additionally to the simulated δ^{18}O concentration in runoff a mean transit time is computed in each time step, making it possible to evaluate the transit time development in conjunction with other hydrological phenomena. The HBV distribution model was tested with two artificial time series, dirac-impulse and sine-shaped input. It proved successful and was then applied in the Brugga and Zastlerbach catchment, two adjacent mountainous forested catchments.

Furthermore, lumped parameter models (EM, EPM) were evaluated with a sine-wave regression in order to compare resulting transit times with the conceptual model simulation.

The HBV model results revealed a clear distinguishable shift of mean transit times in the Brugga catchment in connection with the 2003 drought. That change is also detectable in the isotopic composition of the stream water. The shift is also apparent in the Zastlerbach catchment, but the simulation gives evidence to suggest that the effect already diminishes due to the smaller catchment size.

The absolute HBV-simulated transit times were not considered very trustworthy, because the model is fitted with trial and error and similar looking fits can yield markedly different transit times. The relative development in time, however, is not affected by that uncertainty.

Keywords: δ^{18}O, transit time, conceptual model, lumped parameter model, sine-wave regression, mesoscale catchment.

Zusammenfassung

Das Ziel der vorliegenden Diplomarbeit war die Untersuchung und Bewertung der mittel- und langfristigen Auswirkungen des Trockenjahres 2003 auf zwei mesoskalige Einzugsgebiete im Südschwarzwald. Dazu wurde innerhalb der HBV Modellumgebung ein konzeptionelles Verweilzeitmodell entwickelt und in den Untersuchungsgebieten angewandt.

Als Datengrundlage standen tägliche Zeitreihen des Niederschlags, der Temperatur, der rel. Luftfeuchte und des Abflusses an den Gebietsauslässen sowie Wochenproben von δ^{18}O in Niederschlag und Abfluss zur Verfügung. Die Untersuchungsperiode dauerte von 2000 – 2006.

Der erste Arbeitsschritt bestand aus der Entwicklung eines Verweilzeitmodellkonzeptes, dass sich in die HBV-Struktur implementieren lässt. Die wesentlichen Erweiterungen sind neue Speicherkonzepte, da das Linearspeicherkonzept keine realistische Wassermenge im modellierten Gebiet vorhält. Die erweiterte HBV-Version bietet die Möglichkeit, jedes perkolierende Wasservolumen separat mit dazugehöriger Konzentration und Eintrittszeit zu speichern. Die Verteilung der Abflussbeiträge der nun diskreten Speicherkomponenten kann gleichförmig bis exponentiell verteilt werden. Im letzteren Fall tragen die jungen Speicherkomponenten wesentlich mehr zum Abfluss bei als solche, die länger im Speicher verweilen. Das reflektiert die Annahme einer exponentiellen Verweilzeitverteilung der unterirdischen Fließwege im Einzugsgebiet.

Zusätzlich zur simulierten δ^{18}O Konzentration im Abfluss wird das mittlere Alter des Abflusses berechnet, um die tägliche Entwicklung der mittleren Verweilzeit des Abflusses in Verbindung mit anderen hydrologischen Phänomenen zu erfassen.

Das so angepasste HBV Modell wurde mit künstlichen, idealisierten Datenreihen erfolgreich getestet und anschließend in den Einzugsgebieten der Brugga und des Zastlerbachs, zwei benachbarten montanen, bewaldeten Einzugsgebieten angewandt.

Zusätzlich wurden Sinusregressionen mit den gemessenen δ^{18}O Zeitreihen durchgeführt, um die Ergebnisse des konzeptuellen Verweilzeitmodells zu evaluieren. Es wurde in beiden Einzugsgebieten die mittlere Verweilzeit nach dem Exponentialmodell und dem Exponential-Pistonflowmodell berechnet.

Die HBV Modellergebnisse zeigten eine deutliche Erhöhung der mittleren Verweilzeit im Brugga Einzugsgebiet in Verbindung mit dem Trockenjahr 2003. Diese Änderung wird auch in der δ^{18}O Konzentration des Abflusses sichbar.

Auch im Zastlerbach Einzugsgebiet zeigt sich der Einfluss des Trockenjahres, allerdings zeigt die Simulation Hinweise darauf, dass die Auswirkungen dort bereits am abklingen sind, vermutlich aufgrund der kleineren Einzugsgebietsgröße.

Die absoluten HBV-simulierten Verweilzeiten werden nicht als besonders vertrauenswürdig eingestuft, da die Zeitreihen rein optisch angepasst wurden und sich ähnlich passende Modellanpassungen finden lassen, die aber ein anderes mittleres Verweilzeitniveau erzeugen. Die relative zeitliche Entwicklung bleibt davon aber unberührt.

1 Introduction

1.1 General introduction

Transit time modelling has been and is still an important research field in catchment hydrology. Transit time, the time a water volume spends in a hydrologic system, is an important catchment descriptor because it comprises information about flowpaths and helps understanding various catchment properties. Applications may be solute transport (contamination), recharge and aquifer capacity or more derivately water quality management.

Environmental tracers are commonly used to asses transit times, especially isotopes of the water itself (^{18}O, ^{2}H and ^{3}H), continuously applied to the catchment with precipitation. Different approaches exist to model the transit time.

Generally, transit time modelling is limited by the precision of in- and output data, the choice of a correct distribution model and assumptions on recharge, that have to be taken into account. In order to avoid at least some of these issues and to get an estimation not only of longterm mean transit times but also transit time development during different flow conditions, especially lowflow, the thesis' approach was chosen.

1.2 Objective

The major aim of this thesis is the development of a transit time modelling module which fits into the framework of a working quantitative model (HBV model) and the subsequent application on a mesoscale catchment. The closer objective is to design a tool that reveals information on the development of transit times in stream water during drought conditions and the mid- to long-term influence of droughts on the subsurface watersystem.

The underlying motivation for this approach is to test the possibility to benefit from the conceptual structure of the quantitative model which describes important hydrological processes and catchment components (e.g. gradients of temperature and precipitation, evapotranspiration dependent on season and climatic condition, runoff contribution from soils, aquifer properties) and produce time series of runoff ages along with the modelled runoff. This is primarily accomplished by the integration of a fittable distribution of runoff components from the model's storages.

Additionally, with a sine-wave regession a lumped parameter model is fitted to estimate mean transit time in order to evaluate the results of the conceptual approach.

1.3 Transit time modelling approaches

1.3.1 Stable isotopes in transit time modelling

Generally, the use of stable isotopes, i.e. $\delta\,^{18}O$ and ^{2}H (D) in catchment hydrology can provide valuable information about origin, flow pathways and storage conditions of streamflow components and thus also for transit time estimations. Common approaches are based on lumped parameter modelling (Maloszewski and Zuber, 1982), where mathematical transit time distribution (TTD) models are used to translate an input function (precipitation concentration) into an output (streamflow concentration).

The applicability of the water's stable isotopes is based upon concentration changes in time. Fractionation processes occur due to the different atomic masses of ^{18}O and D compared to the "normal", most abundant isotopes ^{16}O and ^{1}H during phase transitions. They result in a depletion of ^{18}O and D in evaporated and sublimated waters and enrichment during condensation and resublimation. These processes can, from a hydrological point of view, be summarized to several fractionation effects which influence the isotopic composition of precipitation. Those are:

- Continental effect
- Elevation effect
- Latitude effect
- Amount effect
- Temperature effect
- Season effect

The most important effect relating to longtime mesoscaled observations in temperate climates is the elevation effect unless for single storm events the pattern of ^{18}O can differ extensively up to inversion of the common gradient. (Moser and Rauert, 1980; Kendall and McDonnell, 1998).

In conjunction with transit time modelling another important effect besides fractionation is the selection. It describes a "pseudo-fractionating" selective behaviour of components in the hydrological cycle due to other reasons than the difference between the isotopes. An example is the saison-dependent transpiration and its influence on recharge volumes compared to precipitation, which can result in an offset mean isotope composition of groundwater recharge compared to precipitation.

The isotopes of the water molecule are ideal environmental tracers as they consist of water themselves. This and their conservative behaviour in aquifers as well as soils and streams make them reliable tracers for transit time studies that cover all structural catchment parts in most cases. Other environmental isotopes like noble gas isotopes which are applicable in aquifer studies cannot be used here due to their interactions with the atmosphere (McGuire and McDonnell, 2006).

The ^{18}O values in this thesis are presented in the δ notation, the normed difference in sample concentration compared to a standard (V-SMOW).

1.3.2 Transit time distributions and modelling approaches

The transit time distribution (TTD) of a catchment is a hypothetical response function that incorporates all catchment factors which influence a water volume on its way through the reflected system. While theoretically transit time distributions might be time-variant, generally a time-invariance is supposed for transit time estimations and a TTD model is fitted to observed data in order to determine the transit times.

Four common TTD model types exist: piston flow, exponential, exponential-piston flow, and dispersion models. Piston flow models describe no further distribution but an time offset (one parameter). Exponential models describe a exponential pathway distribution, starting without time lag, i.e. a fraction passes the system instantly with the rest following exponentially decreasing (one parameter). Exponential-piston flow models combine these approaches, they are lagged exponential models (two parameters). Dispersion models finally describe a left-skewed distribution implying an advective-dispersive system (three parameters).

Three approaches exist to fit the lumped models, these are: (a) integrating the tracer input function with the TTD, the convolution integral which is solved numerically in the time domain, (b) solving the convolution by transformation of in- and output to the frequency domain, and (c) estimating mean transit times with a sine-wave regression. A sine-wave regression is applied in chapter 6. For a comprehensive overview see McGuire and McDonnell (2006).

Lumped TTD models are undependent of hydro- or meteorological data, which is an advantage compared to conceptual approaches. But they have several limitations, which are easily violated in catchment modeling. These are e.g. input function determination (spatial homogeneity and recharge) or time variance of catchment properties. (Maloszewski and Zuber, 1982; Soulsby et al., 2000; McGuire et al., 2002; Rodgers et al., 2005; McGuire and McDonnell, 2006).

1.4 Conclusions

Several approaches are known to estimate transit times, most of them are based on the assumption of a system-characteristic transit time distribution, to which tracer data can be fitted. For the application of lumped parameter models no further catchment information is needed, but they have limitations that restrict their potential in catchment transit time modelling. Conceptual approaches on the other hand have a high demand of hydrological data.

The objective of the thesis is to estimate mean transit time and transit time development under drought conditions in two mountainous catchments in the Southern Black Forest. Two methods are used to estimate transit times, a conceptual approach based on the HBV model and the assumption of exponential pathway distribution, and additionally a lumped parameter sine-wave regression.

2 Area and investigation period

2.1 The Brugga and Zastlerbach Catchment

2.1.1 Location and morphology

Both Brugga and Zastlerbach are streams within the Dreisam catchment southeast of Freiburg (Br.) in the southern Black Forest. Whereas the surrounding Dreisam catchment shows a distinct morphological division in the mountainous Black Forest parts, mostly forested with meadowy valley bottoms and the Zarten basin, a large plain-shaped valley filled with glacial sediments, mostly agricultural land, the Brugga as well as the neighboured Zastlerbach catchment are situated completely in the Black Forest.

As this particular area has been under investigation by the Institute of Hydrology over the last two decades, with enduring climatological and hydrological routine measurements as well as numerous singular studies, lots of publications and diploma theses have been released with descriptions of the area. Information presented in this section is mainly based on the works by Holocher (1997), Lindenlaub (1998), Uhlenbrook (1999a), Didszun (2000), Wissmeier (2005) and Ehnes (2006). Table 2.1.1 gives some basic geographical informations about the catchments.

Characteristical for the investigated area are deep valleys with steep, forested slopes. The forests' dominating species are Norway spruce and beech. Furthermore, in exceptionally steep parts and below rock outcrops screes and talus fields occur. The geomorphology was shaped by two major influences: the southern parts of both catchments where the highest point is located (Feldberg, 1493 m a.s.l.) were temporarily glaciated during the Würm ice age ($\sim$ 10000 B.P.) and show results of glacial erosion like U-shaped valleys and morraines. The northern parts up to the opening into the Zarten basin never experienced glaciation but were formed under periglacial circumstances (V-shaped valleys and gullying).

2.1.2 Geology and soils

The southern black forest consists mainly of metamorphic bedrocks (e.g. gneiss), which can be considerably jointed, especially in areas of intense tectonical movement. These bedrocks can crop out at the surface, but they are mostly covered with a typical sequence ("‘Periglaziale Deckschichten"’) of Quarternary-developed layers constituting of rock debris, scree and fine material. These developed due to intense weathering and solifluction on the steep slopes under

Table 2.1.1: Geomorphological properties of the investigation area, characteristic parameters.

	Brugga catchment	Zastler catchment
area (km^2)	39.8	17.8
min. height (m a.s.l.)	436	548
max. height (m a.s.l.)	1493	1493
height extension (m)	1057	945
Surface ratio slope angle (%)		
0° - 20°	43	45.3
20° - 40°	47.3	53.8
> 40°	9.7	0.9
Landuse (%)		
urban area	0.9	0.1
agriculture & grassland	22.3	13.8
forest	76.9	86.0

periglacial conditions to a considerable thickness (~ 50 - 150 cm). An ideal sequence starts (from the lower boundary/bedrock) with the Base Layer, due to solifluction horizontally aligned rocks in a dense matrix, followed by the Main Layer with a lower fraction of non-aligned rocks and finally the thinner Topset Layer with an again higher fraction of rocks. However, this scheme is idealized and not every layer might be clearly distinguishable.

At the valley bottom holozene alluvial sediments can be found, in the southern parts also morraine material.

2.1.3 Climatic conditions and hydrology

The regional climate is temperate and influenced by alternating passages of cyclones and anticyclones, driven by the west wind drift. Due to the mountainous relief local climate characteristics show an altitude dependency. During the investigation period (1999-2006), mean annual temperatures at the three meteorological stations (see section 2.2, page 11) are 8.1 °C at the station Schweizerhof (720 m a.s.l.), this station is located in the Zastlerbach catchment, 7.7 °C at the station Katzensteig (775 m a.s.l.), which is situated in the St. Wilhelm valley, one upstream valley of the Brugga catchment, and 6.3 °C on the Schauinsland[1] (1205 m a.s.l.), located on the southwestern edge of the examined area. In wintertime, inversion weather situations frequently occur, resulting in reversed temperature gradients. Figure 2.1.1 shows the annual variation of temperature at the three station sites.

The precipitation in summertime is dominated by convective storm events, whereas in wintertime cyclonal rain- and snowfalls are prevailing. In the higher parts about 37 % of the annual precipitation fall as snow (Trenkle and v. Rudolf, 1989 in Ehnes, 2006). The precipitation in general shows a

[1] only data for Jan. 1999 to Feb. 2004

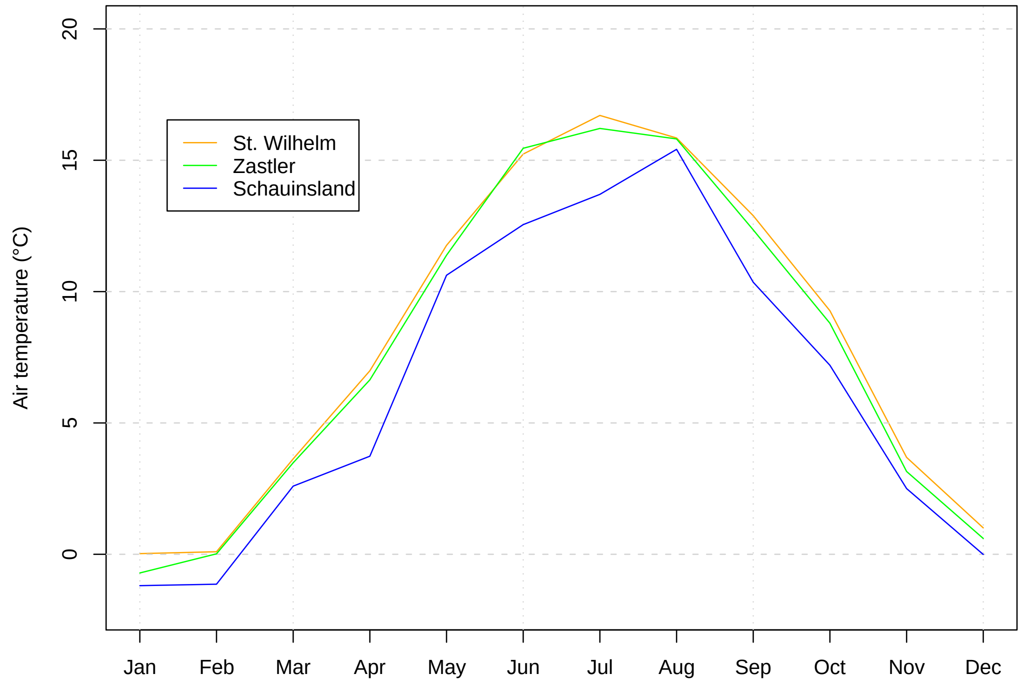

Figure 2.1.1: Monthly mean air temperature at the three stations in the catchments over the investigation period (Schauinsland: 1999-2004).

clear altitude dependency, but is also influenced by the local topography (e.g. luff/lee situations, especially in the higher parts, where precipitation is blown over due to strong winds). Nevertheless, for singular storm events rainfall can show a high variability caused by the wind direction and luff-lee effects like vapor depletion in the clouds (Holzschuh, 1995). Throughout the investigated period the following mean annual precipitation volumes were observed: 1490 mm at the station Schweizerhof, 1557 mm at the station Katzensteig, 2117 mm on the Schauinsland. In Figure 2.1.2 the monthly mean sums at the stations are illustrated.

The potential evapotranspiration ETP$_{Haude}$ (calculated with the Haude formula (DVWK, 1996)) shown in Figure 2.1.3 as mean daily values on a monthly basis average to 401 mm (Schweizerhof), 520 mm (Katzensteig) and 336 mm (Schauinsland). There is no obvious explanation for the strong deviation between Schweizerhof and Katzensteig as they are approximately on the same elevation level. Nevertheless, it can be stated that a) the time series is not that long, so one could expect some scatter in the averages, b) these are spot measurements which do not integrate regional variations, c) evapotranspiration in this area is mainly limited by humidity, which might be more often close to 100 % due to local specialities, e.g. exposure.

The hydrogeologic characteristics of the bedrock show strong variations in the area, as the metamorphic rock itself can be considered non-porous, the decisive property is the joint system which varies considerably and causes variations in hydraulic conductivity from 10^{-10} to $10^{-5}\frac{m}{s}$ and decreases with depth

(Stober, 1995).

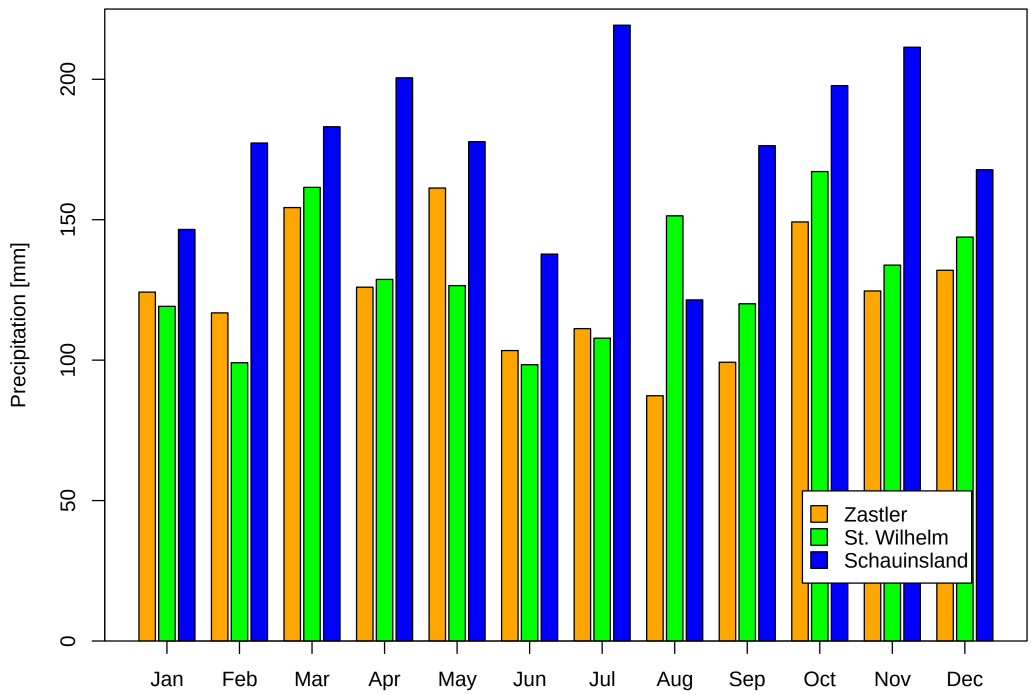

Figure 2.1.2: Monthly mean precipitation sums at the three stations in the catchments over the investigation period (Schauinsland: 1999-2004).

The unconsolidated top layers with high conductivities and their potential to store fast exchangeable water are of great importance for mid-flow and flood runoff, which mobilizes rapidly under rainfall conditions (Uhlenbrook, 1999a). Table 2.1.2 shows some longterm runoff characteristics for the Zastler Bach and Brugga catchments. The runoff regime is pluvio-nival, in Figure 2.1.4 two peaks can be seen, one minor autumn rainfall peak and a major spring peak, caused by snowmelt and rainfall. The minimum runoff occurs in the late summer, before the refilling of the storages begins.

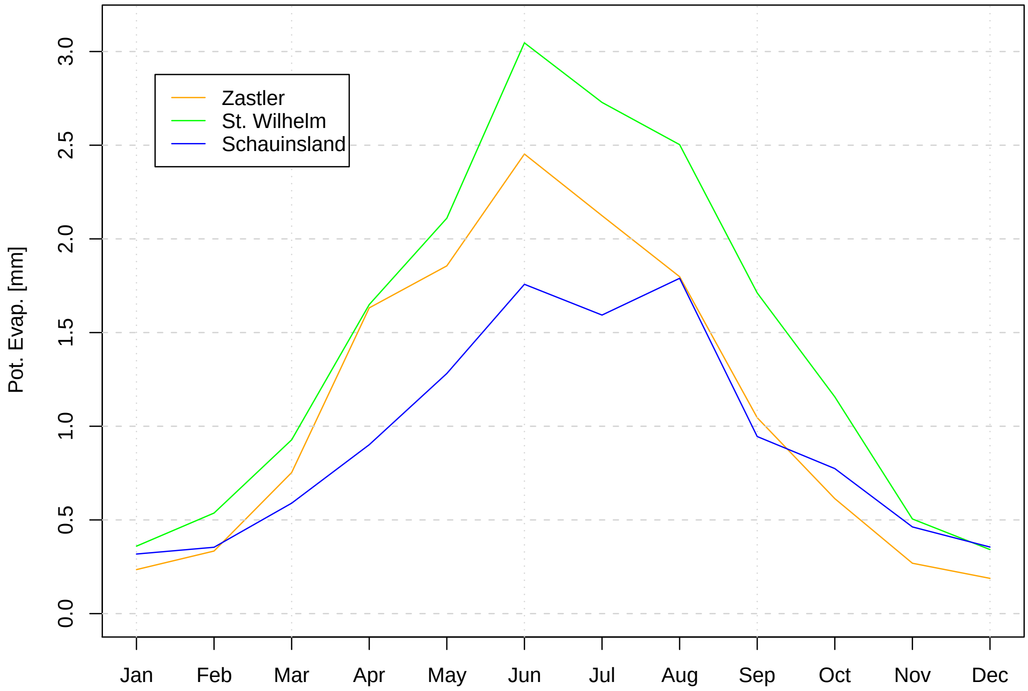

Figure 2.1.3: Daily potential evapotranspiration (after Haude), averaged by month at the three stations over the investigation period (Schauinsland: 1999-2004).

Table 2.1.2: Runoff characteristics at the gauging stations, runoff (*Q) in $\frac{m^3}{s}$, specific runoff (*q) in $\frac{l \cdot km^2}{s}$ (LfU, 2000 in Wissmeier, 2005).

	Brugga catchment	**Zastler catchment**
time series	1934-1994	1955-1994
HQ	33.61	24.37
MHQ	15.75	6.86
MQ	1.54	0.63
MNQ	0.37	0.13
NQ	0.19	0.06
MHq	442	385
Mq	39.1	35
MNq	9.03	7.3

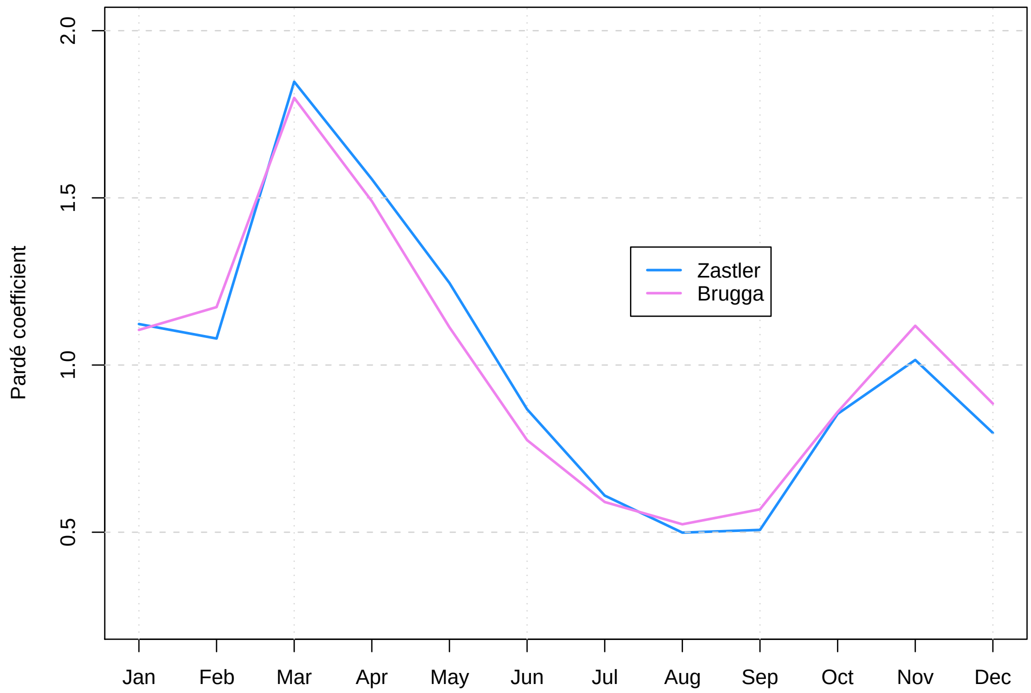

Figure 2.1.4: Runoff regime at the outlets of Brugga and Zastler, calculated from investigation period data.

2.2 Data

2.2.1 Data sampling

The investigation period which was finally modelled with the modified HBV model lasts from January 2000 to October 2006. Data series taken for gradient or runoff regimes partly covered longer periods which were then accepted for calculations where possible.

Isotope ratios and most meteorological data presented and interpreted in this thesis (including $\delta\ ^{18}O$ samples) originate from longterm routine measurements of the Institute of Hydrology carried out in the catchment of the nearby Dreisam and its contributing substreams respectively. Two climate observation stations, valley bottom located (see also section 2.1.3), provided temperature and precipitation volumes in form of daily means and sums respectively. Furthermore, 2:00 p.m. humidity values from the stations were introduced for potential evapotranspiration calculation.

For the calculation of temperature and precipitation gradients, time series from the DWD climate station Schauinsland were available, they lasted from January 1999 to January 2004.

Runoff time series at the catchment outlets were measured by the Landesanstalt für Umweltschutz (LfU) as gauge heights and converted to discharge with spot-measurement based gage-runoff relations also provided by the LfU.

$\delta\ ^{18}O$ sampling was taken out approximately weekly over the study period. The precipitation concentrations were measured from bulk samples collected in a Hellmann precipitation collector and thus represent a mean value over the space of time since the beforehand sampletaking, whereas the streamflow values are to be understood as snapshots as they were measured from sample volumes taken directly out of the stream on the respective day.

$\delta\ ^{18}O$ snow samples from the work of Ehnes (2006) were utilized for the discussion of the model results. A gradient of $\delta\ ^{18}O$ in precipitation was calculated from event measurements taken out in the area by Holzschuh (1995).

2.2.2 Data processing and transformation

Potential evapotranspiration (ETP) was needed as input for the HBV model and calculated as a monthly day-mean with the Haude formula (2.2.1) (Haude factors see table 2.2.1). Because radiation measurements were not available from the station Schweizerhof, the computation of more complex ETP models was impossible. But since the values were mainly calculated as input for the HBV model, which effects a generation of uncertainty anyway (e.g. transfer spot measurement to area), this was considered admissible.

The ETP$_{Haude}$ is calculated with 2:00 p.m. measurements and is an empirical function of the vapor pressure deficit:

$$ETP_{Haude} = f \cdot (e_s(T) - e)_{14} \leq 7\frac{mm}{d} \qquad (2.2.1)$$

	Jan	Feb	Mar	Apr	Mai	Jun	Jul	Aug	Sep	Oct	Nov	Dec
f_d	0.22	0.22	0.22	0.29	0.29	0.28	0.26	0.25	0.23	0.22	0.22	0.22
f_m	6.82	6.22	6.82	8.70	8.99	8.40	8.06	7.75	6.90	6.82	6.60	6.82

Table 2.2.1: Haude factors for days (f_d) and months (f_m) (from DVWK, 1996)

Therein the vapor pressure deficit e_s(T)-e:

$$e_s(T) - e = e_s(T) \cdot (1 - \frac{U}{100}), \tag{2.2.2}$$

where U is the humidity (%) and e_s(T) is the saturation vapor pressure, which is determined from the air temperature (T) with the Magnus formula (coefficients after Sonntag, valid between $-45 \leq T \leq 60$ (°C)):

$$e_s(T) = 6.11 \cdot \exp^{\left(\frac{17.62 \cdot T}{243.12+T}\right)} \tag{2.2.3}$$

The resulting values are shown in the preceeding section on page 9 (figure 2.1.3).

The HBV model was used with different elevation zones, so gradients for precipitation and temperature had to be parametrized for the examined period of time. Linear regressions of the daily precipitation time series between the "‘valley bottom stations"’ Schweizerhof and Katzensteig and the Schauinsland station were calculated for days with precipitation at both stations (Figure 2.2.1, 2.2.2). Because of the small difference in elevation between Schweizerhof and Katzensteig (δh: 55 m) the scatter due to other influences like local precipitation variation was relatively strong and thus the correlation too weak to give reliable results and the regression was neglected.

Analogous, regressions for air temperature (Figure 2.2.3, 2.2.4) were computed. A linear regression model of the form $y = a \cdot x$, i.e. a y-axis intercept was prevented for the precipitation because of the assumption that no precipitation at one station should not imply rainfall at the dependent one. This limitation was not necessary for the temperature regression, so the regression model here was of the form $y = a \cdot x + b$.

Holzschuh (1995) sampled seven precipitation events at several heights and calculated $\delta\,^{18}$O gradients from the measured concentrations. The investigation was carried out from October to December 1994 and covered rainfall events of different duration and intensity and one event with a mix of rainfall, snow and hail. The gradient regressions were never too weak, but also never excellent. The R^2 ranged from 0.59 to 0.77. However, the resulting gradients vary from -0.14 to -0.38 ‰ per 100 m, which is quite a lot, even more when considering the fact that the events only covered the autumn rainfall season and might have little significance for e.g. convective summer storm events. Nonetheless, a mean was calculated and taken for precipitation concentration correction later on. The final gradient then was -0.23 ‰ per 100 m which is in range of literature values (2 to 4 ‰ per 100 m, Moser and Rauert (1980)) and thus accepted despite the above mentioned uncertainty.

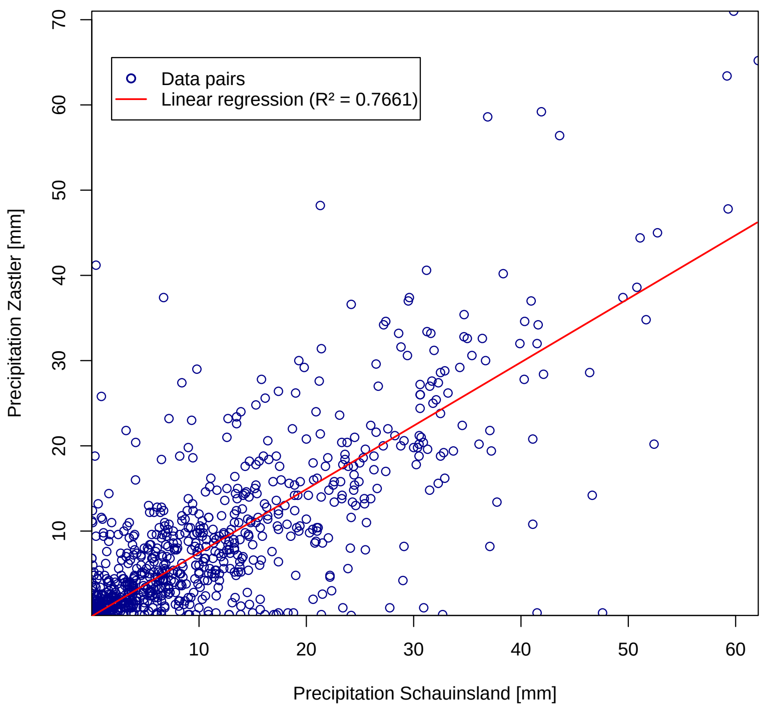

Figure 2.2.1: Precipitation gradient regression between Schauinsland and Schweizerhof.

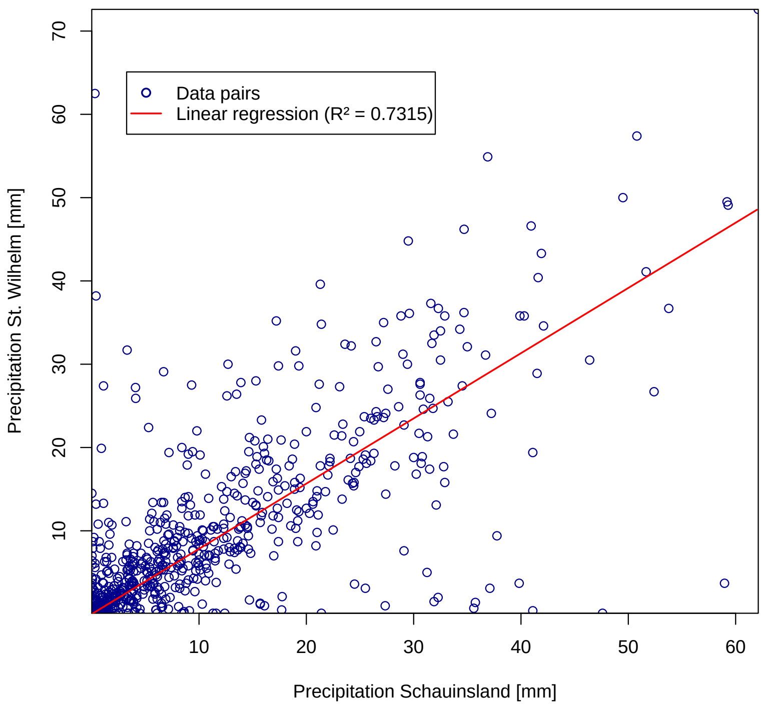

Figure 2.2.2: Precipitation gradient regression between Schauinsland and Katzensteig.

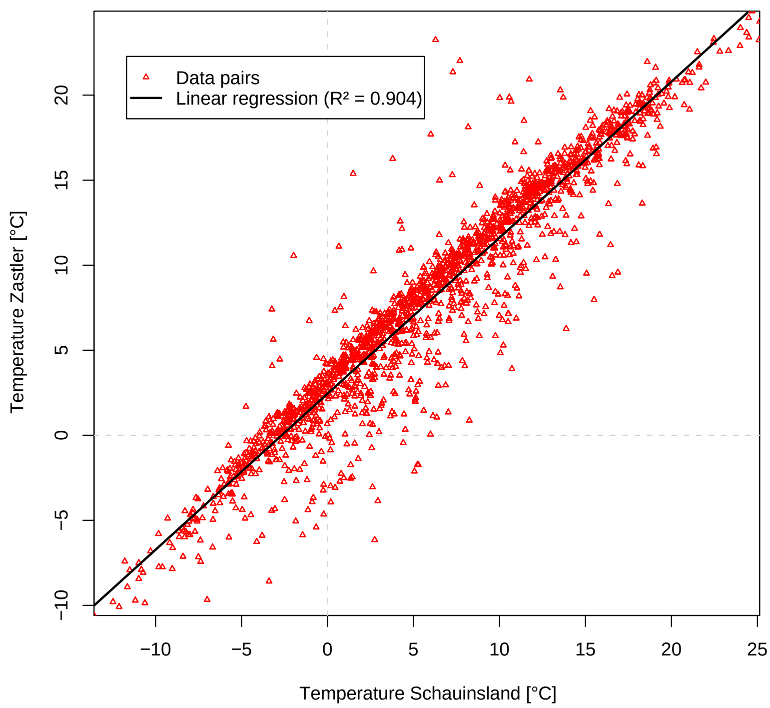

Figure 2.2.3: Temperature gradient regression between Schauinsland and Schweizerhof.

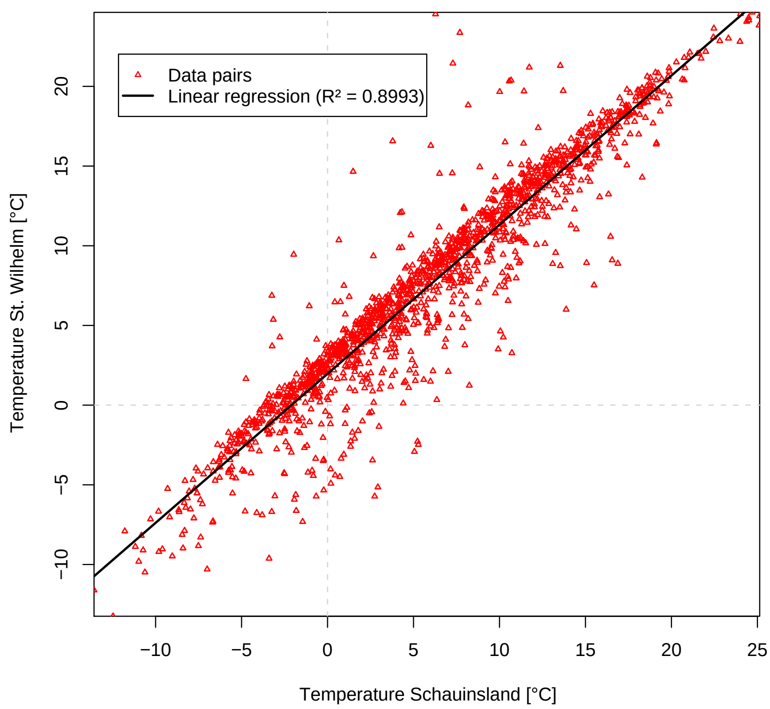

Figure 2.2.4: Temperature gradient regression between Schauinsland and Katzensteig.

Table 2.2.2: Regression results and gradients, "final" rows contain the gradients (per 100 m) used later on. Further explanation see text.

	a	b	R^2	δh	gradient
Precipitation regression					
Schau. ~ Schweizerh.	0.7452	0	0.77	485 m	7.05 %
Schau. ~ Katzenst.	0.7831	0	0.73	430 m	6.44 %
final					6.75 %
Temperature regression					
Schau. ~ Schweizerh.	0.9173	2.4442	0.90	485 m	-0.279 °C
Schau. ~ Katzenst.	0.9355	1.9680	0.90	430 m	-0.209 °C
final					-0.244 °C
Precipitation δ ^{18}O regression					
min	-0.0014	-12.401	0.77		-0.14 δ ^{18}O
max	-0.0038	-8.173	0.59		-0.38 δ ^{18}O
final					-0.23 δ ^{18}O

All above discussed regression results and consequential gradients are summarized in table 2.2.2.

Input time series of temperature, precipitation, runoff and $\delta^{18}O$ concentrations in precipitation and runoff were needed for the model. The HBV model is capable of correcting temperature and precipitation model-intern with given gradients and a set of elevation zones (for more detailed explanations see chapter 3). But this does not apply for the newly implemented model parts. Thus, the precipitation concentrations have to be passed to the model in a corrected form. Although the spatial patterns in $\delta^{18}O$ concentration of single storm events certainly were various (see section 1.3.1), the longterm mean input concentration will definitly diverge from the values measured at the meteorological stations located on the valley-bottom. That is why an longterm elevation gradient in $\delta^{18}O$ was accepted as a trade-off.

For this purpose a corrected δ^{18}O concentration mean (δ_{corr}, equation (2.2.4)), weighted by area fractions of the elevation zones and elevation gradients of precipitation and δ^{18}O, had to be calculated from the measured values:

$$\delta_{corr} = \sum_{i=m}^{n} (\delta + i \cdot G_\delta) \cdot (1 + i \cdot \frac{G_P}{100}) \cdot a_i \quad , \quad \sum_{i=m}^{n} a_i = 1 \qquad (2.2.4)$$

Therein is δ the station measured δ^{18}O concentration, i the counting variable in the boundaries of m and n, with m representing the lowest elevation zone (each zone of 100 m height extent) counted from the zone in which the measurements were taken out (e.g. -2) and n the upper zone respectively. G_P (%/100 m) and G_δ (‰/100 m) are the gradients of precipitation and δ^{18}O concentration, a_i are the area fractions of the elevation zones. In Figure 2.2.5 the corrected and uncorrected precipitation δ^{18}O is plotted.

For the uncorrected δ^{18}O concentrations means are taken from the stations Zängerlehof and Katzensteig if both values are available. Otherwise the measured value from one station is taken unchanged. This occurred particularly

Figure 2.2.5: Precipitation δ^{18}O in the Brugga catchment, corrected and uncorrected.

in wintertime. This time series of δ^{18}O was then taken as raw input for both catchments but subsequently corrected individually according to the respective elevation distributions.

2.3 Conclusions

The two investigated mesoscale mountainous catchments are located in the Southern Black Forest, southwestern Germany. The climate is temperate with yearly precipitation sums of approximately 1500 to 2000 mm. The geology is dominated by metamorphic bedrocks with unconsolidated toplayers. The area was partly glaciated during the last ice age. The catchments have been under investigation repeatedly by the Institute of Hydrology at Freiburg Unversity and longterm measurement data series have been collected.

Time series of precipitation and temperature from three stations were used to calculate elevation gradients. Time series of runoff, calculated from pressure gauges were available as well as weekly δ^{18}O values for both precipitation and streamwater. The investigated period lasted from 2000 to 2006.

3 Introduction to the HBV model

3.1 General description

The HBV model was originally developed at the Swedish Meteorological and Hydrological Institute, SMHI in the early 1970s. It has been widely applied for runoff simulations all over the world, but particulary in catchments with temperate/cold-temperate climatic conditions with at least partly forested areas. Also, it has influenced a number of succeeding models which incorporated e.g. different snow routines. Known applications of the model cover a catchment size of less than one up to 40 000 m^2. This wide adaptability is owed to the relative simplicity of the model structure, making the model general (Bergström, 1995). Holocher (1997) applied the HBV model in the Brugga and a nested subcatchment (St. Wilhelmer Talbach) and stated good adaptability of the model ($R_{eff} \sim 0.85$) for this area.

Generally, the model simulates catchment properties with a lumped approach, the used version offers at least partly distributed simulations, in terms of landcover- and elevation zones (see Section 3.2). Discharge is computed from time series of precipitation and potential evapotranspiration (ETP) in a sequence of modules, which are (in order from the entering of a precipitation volume): a day-degree snow routine, a soil moisture routine, a response function (based on the single linear store, SLS) and finally a routing routine in form of a weighted distribution function.

The version used in this thesis is the “HBV light”, a GUI front-end program written in Visual Basic 6 by Jan Seibert. It offers several alternative model structures (e.g. different lumped/distributed choices, one/two/three groundwater boxes) as well as additional input possibilities like long-term daily mean temperature values for ETP correction or gradient series of precipitation and temperature instead of constant values. Additionally, an optimation algorithm is integrated to the model.

The following section gives a short overview over the model’s properties and parameters as well as the required data. For a more comprehensive description refer to Seibert (2002), where the following section is excerpted from.

3.2 Model version

3.2.1 Modules

In the following a short description of each model routine (only for the version which was altered then for transit time computations) is given, including the related parameters. An illustrating figure can be found in chapter 4.3, page 29. Although it shows the modifications for the transit time calculations the basic model structure is obvious.

Snow routine: Precipitation is classified as snow below a certain threshold temperature T_T, then volume corrected by multiplication with a correction factor SFCF and accumulates in a separate box. During melting conditions (temperature above T_T), the melting volume is calculated by a simple degree day method via a degree-day-factor C_{FMAX}, which is retained in the snow up to a certain amount (C_{WH}, in % of the snow pack's water equivalent) and finally enters the next routine. When returning to freezing conditions from a melting phase, the retained water partly refreezes, controlled by a refreezing factor C_{FR}. These calculations will be carried out separately for possible set elevation and landuse zones.

Soil routine: The most important remark on the HBV's soil routine with respect to the implementation of the transit time modelling routine is that it behaves like a dead end street for the percolating precipitation (resp. snowmelt) and serves only as a reservoir for evaporable and transpirable water (both simplifying and limiting). The soil-contributed discharge is thus integrated in the next routine. The soil's maximum capacity is defined by the maximum soil moisture storage FC (no indicator for real-life field capacities of the soils in the catchment). The percolating water is divided into one part filling the soil storage and another entering the runnoff routine. Depending on the soil storage charge the relative contribution is determined by a power function with the parameter β in the exponent. Evapotranspiration is determined by a soil moisture value LP (relative charge compared to FC). It ranges from potential evapotranspiration ($\frac{charge}{FC} \geq LP$) to zero, reduced by a linear function if $\frac{charge}{FC} \leq LP$. This routine can be computed separately for landuse and elevation zones as well.

Runoff routine/response function: DHere, only the properties of the chosen model version are described (several exist, see section 3.1). The response function consists of two storage components of which the upper one receives all recharging water and then transfers a fixed amount PERC into the lower one. In the next step, runoff is generated. While the lower storage SLZ is a basic single linear storage (SLS) with runoff proportional to the storage volume: $Q_2 = K_2 \cdot SLZ$ (K_2: runoff coefficient), the upper storage's runoff grows disproportional with increasing storage volume, triggered by a second parameter α: $Q_1 = K_1 \cdot SUZ^{\alpha}$. This results in a relatively higher runoff contribution from the upper storage on higher storage volumes. The upper storage has no volume limitation and in modeling practice generates the quick runoff reaction on a storm event. The lower storage often has an about one decimal power smaller runoff coefficient and is mainly responsible for longterm baseflow runoff. Calculations in this routine are always performed in a lumped way.

Routing routine : The runoff generated in one timestep is not directly passed to the outlet, but distributed onto the next days, given by parameter MAXBAS, and then weighted by an equilateral triangular function over this number of days.

In total there are 13 parameters to fit a lumped model: five for the snow routine (T_T), C_{FMAX}, SFCF, C_{WH}, C_{FR}), three for the soil (FC, LP, β), four for the runoff routine (PERC, α, K_1, K_2) and one for the routing (MAXBAS). If modelling semidistributed, the parameter sets for snow and soil can be chosen up to three times, one for each landuse zone and they are supplied with different input for each elevation zone (up to 20). Additionally, gradients for precipitation PCALT and TCALT have to be chosen, usually regression slopes over the modelled time series or other longterm means. This sums up to a total of 31 parameters for the semidistributed model.

The model does not need initial values to start a model run. Instead, a "warm-up" phase, typically one year or longer, is used to fill the modules with sufficient volumes. The objective functions skip this phase for evaluation.

3.2.2 Data requirements

First of all, time series of precipitation and temperature are needed, also runoff measurements at the outlet in order to fit and evaluate the model. All calculations are carried out in a regionalized form, so information about (sub-) catchment sizes are mandatory. Unlike precipitation which is typically logged in (mm), runoff measurements often have to be transformed from ($\frac{m^3}{s}$) to specific runoff (mm).

Furthermore, values of potential evapotranspiration, either twelve monthly values or 365 daily values have to be passed to the model. Additionally, a longterm mean temperature value can be read into the model, likewise in a monthly or daily form, by which deviations between measured and mean temperature are determined and used to correct the actual evapotranspiration.

When modelling semidistributed, gradients of precipitation and temperature are mandatory, either as constant values or one value per day.

3.2.3 Model evaluation: objective functions

Even though the value of an "optical fit" should not be underestimated, especially when there are reasons to distrust some measurements (e.g. snow precipitation, frosted gauges etc.), and definitly represents the ultimate decision-aid whether to accept or discard a model fit, some objective functions are helpful to find and legitimate final results. Moreover, they are necessary for the use of optimisation algorithms as indicators of quality.

HBV light offers five objective functions to evaluate a model run. The most common function to estimate the predictive power of hydrological models is the Nash-Sutcliffe efficiency coeffient R_{eff} (equation (3.2.1)). It compares the deviation of modelled and observed runoff volumes with the deviation of the runoff timeseries' mean and the observed value. A R_{eff} of zero means that the model is as good as the mean value. A value of one would be the perfect fit.

$$R_{eff} = 1 - \frac{\sum(Q_{obs} - Q_{sim})^2}{\sum(Q_{obs} - \overline{Q_{obs}})^2} \tag{3.2.1}$$

Quite similar to the R_{eff} is the $\log R_{eff}$ (equation (3.2.2)) which does the same as the former function, but with logarithmized runoff volumes. This causes an accentuation of lower values and thus evaluates the model quality in mid- and lowflow condition.

$$logR_{eff} = 1 - \frac{\sum(\ln Q_{obs} - \ln Q_{sim})^2}{\sum(\ln Q_{obs} - \overline{\ln Q_{obs}})^2} \tag{3.2.2}$$

Also, the (uncorrected) Coefficient Of Determination r^2 is provided (equation (3.2.3)). It describes the proportion of variability that is explained by the regressor (observed runoff) in relation to the model value's total variability. It varies between zero and one.

$$r^2 = \frac{\sum\left((Q_{obs} - \overline{Q_{obs}})(Q_{sim} - \overline{Q_{sim}})\right)^2}{\sum(Q_{obs} - \overline{Q_{obs}})^2 \sum(Q_{sim} - \overline{Q_{sim}})^2} \tag{3.2.3}$$

Another possibility is to compute a weighted R_{eff}, where a weighting function (discrete values in the form: runoff volume $\Rightarrow$ weight) is applied to emphazise a certain system state (e.g. lowflow).

For every model run also the mean difference between simulated and observed runoff per year (meandiff) is computed, which is an important check value if one would like to use the model results for water balance calculations.

3.3 Conclusions

The HBV model, widely applied in humid temperate areas since its development in the 1970s, is a conceptual rainfall runoff model. In the version used here it computes runoff from input data of precipitation, temperature, potential evapotranspiration, and catchment properties. It comprises a snow module, a soil module, and two storages which produce runoff.

4 The conceptual transit time model

4.1 The single linear storage

As described in the preceding chapter the runoff formation in the HBV is modeled by a combination of single linear storages (SLS). The SLS is a key concept in hydrological modeling and describes a runoff Q which is directly proportional to the stored volume S:

$$Q = \frac{S}{k} \tag{4.1.1}$$

with the storage's runoff coefficient k. The mass balance equation for the SLS is then

$$\begin{aligned} p \cdot dt + Q \cdot dt + dS &= 0 \\ \Rightarrow \qquad \frac{dS}{dt} &= p - Q \end{aligned} \tag{4.1.2}$$

where p is the input to the storage volume. The rate of change of storage in time (dS/dt) equals the difference of in- and outflow (p-Q). In the following, p will be assumed to be an instantanious input at the beginning of a regarded period of time.

The following equation is obtained by inserting Equation (4.1.1) in Equation (4.1.2):

$$\frac{dQ}{dt} = \frac{p - Q}{k} \,, \qquad \alpha = \frac{1}{k} \tag{4.1.3}$$

For the initial filling the input function p behaves like a constant. Thus, Equation (4.1.3) is a differential equation of the type $u' = l + ku$, constant k and u, with the analytical solution:

$$Q(t) = \frac{p}{k} \cdot e^{-\frac{t}{k}} \tag{4.1.4}$$

And as p in this particular case is the storage at $t = 0$, S_0, the first factor can be replaced by Q_0:

$$Q(t) = Q_0 \cdot e^{-\frac{t}{k}} \tag{4.1.5}$$

For the discharge at the storage's mean residence time $Q_{T_{1/2}}$applies:

$$\frac{Q_{T_{1/2}}}{Q_0} = \frac{1}{2} \tag{4.1.6}$$

With this, Equation (4.1.5) can be changed to obtain the mean residence time $T_{1/2}$:

$$\begin{aligned} \frac{1}{2} &= e^{-\frac{T_{1/2}}{k}} \\ \Leftrightarrow \qquad T_{1/2} &= \ln 2 \cdot k \end{aligned} \tag{4.1.7}$$

(Modified after Dyck and Peschke (1995), Courant and Robbins (2000), Beven (2001).) In the HBV model the SLS is computed with a discrete recursive function (4.1.8), following the timesteps of the input series.

$$Q_i = \alpha_M \cdot S_i \; , \qquad S_i = S_{i-1} - Q_{i-1} + N_i \tag{4.1.8}$$

Therein, N_i is the input to the storage (at the beginning of each timestep) and α_M the model runoff coefficient.

4.2 Modifications for the integrated ^{18}O transport model

4.2.1 Descriptive introduction

When analyzing the two storages in the HBV model regarding their behaviour in a transport model, one can quickly see that they behave like good mixing reservoirs. The storage volumes in the model are single variables, from which the in- and outputs are added and substracted. Thus, a concentration carried along with an input amount in the original model would have to be mixed out into the storage instantly, altering the overall storage concentration by that. As this behaviour does not match the ideas of transit time distributions stated in section 1.3.2, modifications had to be made in order to integrate a distribution model into the storages.

A major issue with the usage of the HBV's SLS concept for solute transport is that the stored volume which the runoff is composed of is far to small regarding the amount stored in soils and aquifers in the modelled catchments. In the Brugga catchment for instance, mean volumes of the two storages in the HBV's runoff routine were $\sim$ 6 mm and $\sim$ 34 mm respectively for the modelled period. With a mean runoff of $\sim$ 1 and $\sim$ 2.5 mm this corresponds to a mean turnover time of approximately 11.5 days. Of course this is only a very rough approximation, because there are phases with higher storage fillings, but the problem is sufficiantly illustrated: the turnover time of the SLS concept is far to show to match reality – a general design problem of the SLS. It does not help to make the runoff coefficient smaller even though it would enlarge the stored volumes, because that also prevents the model from producing fast and strong runoff reactions to storm events as the relative input amount would decrease proportionally under that condition.

Because of this problem a second modification in the runoff routine was made. Below the storage volume which is the base of the calculation of the

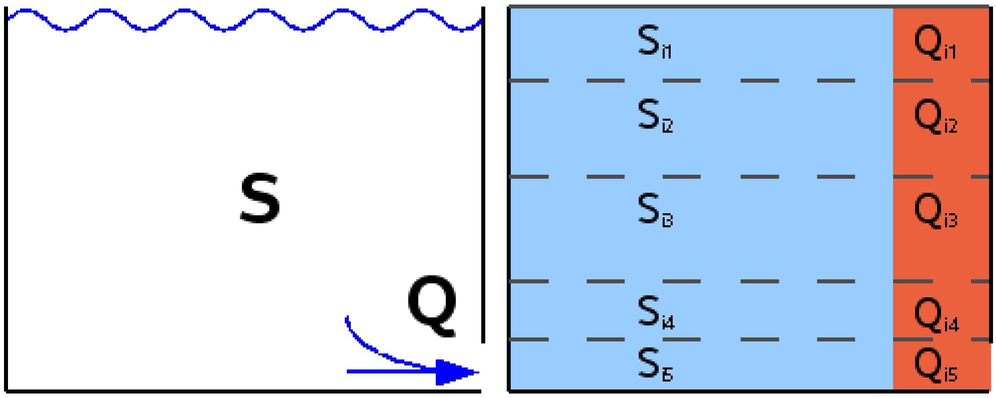

(a) graphical SLS

(b) SLS components at timestep i incl. Good mixing runoff

Figure 4.2.1: The SLS' native behaviour on runoff generation.

runoff reaction, the "active" storage, a second volume was integrated. This so called dead storage does not influence the runoff volume computation but is taken into account when the runoff is distributed on the storage components. It has to be filled before the storage can generate runoff and is refilled from the active storage. This is similar to the modifications Lindström and Rodhe (1986) made within the PULSE model, a model closely related to and derivated from the HBV model, when modelling stream δ^{18}O in small headwater catchments. However, in the modified PULSE model good mixing in the aquifer was assumed, as the modelled areas were small headwater catchments with shallow storages.

4.2.2 Derivation of the distribution model

The storages in the HBV model are filled with recharge on a daily base, in the modified transit time version with a δ^{18}O concentration alongside. So it is possible to track the individual recharge volumes by keeping them separate in a storage-array instead of summing them up to a single storage volume S. When runoff is generated, the storage components natively would contribute each the same fraction α_M of their volume (see figure 4.2.1), analogous to the whole storage (Equation (4.1.8)), at each timestep i and in each component j:

$$Q_{ij} = \alpha_M \cdot S_{ij} \tag{4.2.1}$$

This behaviour was changed to a exponential shaped distribution scheme that represents (a) the distance distribution from cathment surface to stream channels and (b), more important, the distribution of flowpath-length and -velocity (i.e. hydraulic conductivity) with increasing depth (see figure 4.2.2). The storage volume can be regarded as a rectangular function $f(x) = 1$ within the boundaries $x = 0$ and $x = h_i$, with the storage fill height h$_i$ at timestep i. The function has the value one because precipitation and also recharge

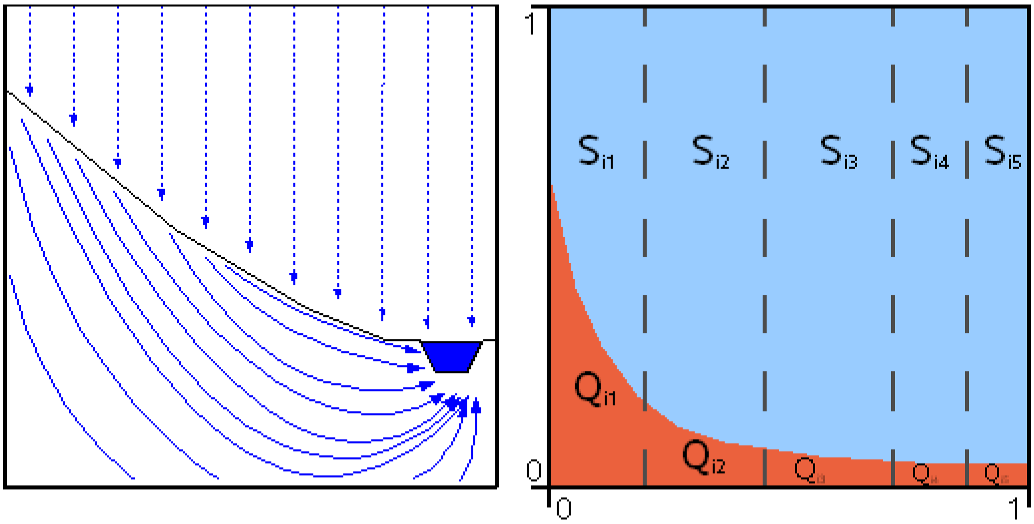

(a) Model idea: exponential pathway distribution **(b)** normalized SLS incl. redistributed runoff components

Figure 4.2.2: Flowpaths and modelled storage.

and runoff are computed as specific volumes ($l/m^2 == mm$). As this is a discrete function with components h_{ij}, any distribution with different α_{Mj} could be applied to it in principle. Nevertheless, one would face problems due to the temporal incontinuity of the storage; the storage filling varies in time and thus no constant segmentation exists. Also, considering the fact that the final storage construction used in this thesis easily consists of several hundred components which would have to be parametrised with each an own α, makes this solution impossible as it would consume so many degrees of freedom, that any result would be hard to legitimate.

Therefore, stricter assumptions based on hydrological hypotheses had to be made. According to the exponential flowpath distribution each amount of recharge reaching the deeper soil and aquifers will be split into different flowpaths with different transit times. The pathway transit times are understood to be exponential distributed. This also implies that an imagined water volume which already has "travelled" a long time through the catchment will not contribute as much as a very recently introduced volume. In an ideal, homogeneous storage, this distribution would be characteristic for all fill heights and also temporarily invariant. So there are basically two assumptions: (a) the exponential distribution in transit times and (b) the assumption of homogenity and time-invariance.

Accordingly, an exponential distribution function had to be found, which can be fitted to match the characteristic runoff contribution scheme outlined above. Ideally, the function should be able to reproduce the SLS native good mixing runoff for intercomparability (a simple x-axis parallel $f(x) = \alpha_M$) and also allow to model with any runoff coefficient α_M given by the quantitative model, i.e. cover the whole storage (rectangular function) as upper extreme value($f(x) = S_{NORM_i}$). This objective was achieved by normalizing the storage volume S to a total volume of one at each time step i, by that creating a rectangular function S_{NORM}:

$$f(x) = S_{NORM_i} = \begin{cases} 0 & \text{for } x \leq 0 \\ 1 & \text{for } 0 < x \leq 1 \\ 0 & \text{for } x > 1 \end{cases} \tag{4.2.2}$$

Now a function has to be found that integrates the runoff Q within the storage and is fittable to different distribution loadings with an emphasis on the younger storage parts. This is indicated in Figure 4.2.2(b). With a standard exponential function:

$$f(x) = \kappa \cdot e^{-\beta x} \tag{4.2.3}$$

where κ is the y-axis intercept, $\alpha_M < \kappa \leq 1$, and β controls the curvature of the function, a variable and thus fittable runoff integral can be spanned over the normalized storage "surface". In order to do this the function has to be integrated within the limits 0 and 1.

$$\int_0^1 \kappa \cdot e^{-\beta x} dx = -\frac{\kappa}{\beta} \left[e^{-\beta x}\right]_0^1 \tag{4.2.4}$$

If β in Equation (4.2.3) approaches 0, the function value within $0 < x \leq 1$ converges to κ, $\lim_{\beta \to 0} f(x)|_0^1 = \kappa$. This then matches explicitly the above mentioned straight horizontal line, making it possible to fit the runoff distribution between a good mixing and a strong curvilinear exponential function. Figure 4.2.3 illustrates some parameter combinations.

The runoff-integral, Equation (4.2.4), must have exactly the same area as α_M, the model's runoff coefficient.

$$\kappa = -\frac{\beta \cdot \alpha_M}{e^{-\beta} - 1} \tag{4.2.5}$$

Because of that one distinct κ exists for every chosen β and vice versa. The distribution model introduces only one additional model parameter (Equation (4.2.5)).

In the programmed model the recharge volumes are stacked in an array. Additionally two arrays with δ^{18}O concentrations (‰) and volume ages (days) are computed alongside, and in each timestep the updated storage array is normalized to a sum of one. Then the distribution function is calculated. Runoff from every component j in the cumulated distribution storage $S_{NORMCUM_j}$(entry in the volume array) is then computed by:

$$Q_{NORM_j} = -\frac{\kappa}{\beta} \left(e^{-\beta x_o} - e^{-\beta x_u}\right) \tag{4.2.6}$$

where x_u and x_o are the lower and upper boundaries of each component j in $S_{NORMCUM}$. The resulting array is then multiplied with the storage vector and

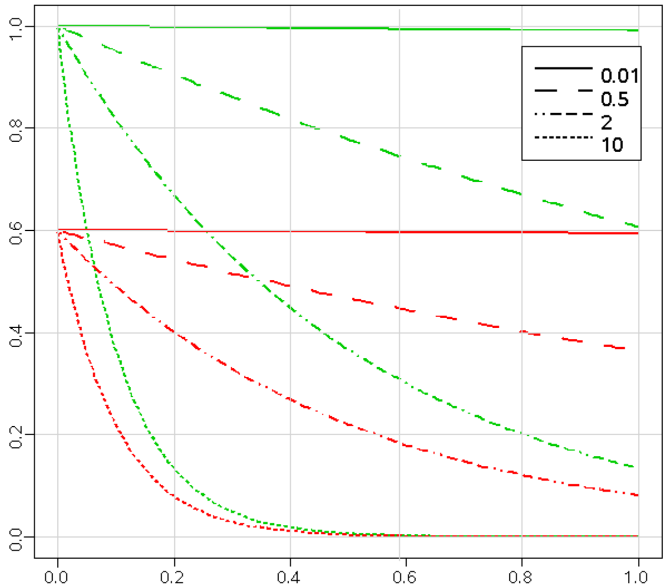

Figure 4.2.3: The distribution function for several β, green: $\kappa = 1$, red: $\kappa = 0.6$.

added up to give the runoff at the respective timestep. δ^{18}O concentration and age are then computed as weighted means.

The model structure is exemplarily shown in Figure 4.2.4, to be read from left to right, starting with the recharge time series R, continuing with the storage computations and ending with the runoff from the storage.

This storage based transit time distribution has been implemented into both storages in the HBV model. Additionally, a second modification was made. As stated in the preceeding section (4.2.1, page 22) the volume stored in a SLS is far to low to represent reality. Accordingly, a dead storage component S_d was introduced as second distribution model parameter and for runoff volume computations subtracted from the total storage volume S (Equation (4.2.7)). This was done analogous to Lindström and Rodhe (1986), but not with the exact same hydrological interpretation. They assumed the dead storage to represent deep well mixed groundwater, which contributes an approximately stable δ^{18}O concentration and thus damps the runoff. In the here presented model structure with dead storages in both fast and longterm runoff generating storages, it has to be regarded more generally as tool to introduce older waters to runoff composition. E.g., it also reflects piston flow effects. Nonetheless its volume also controls the damping here.

$$\begin{aligned} S_{act_i} &= S_i - S_{dead} \\ \Rightarrow \qquad Q_i &= S_{act_i} \cdot \alpha_M \end{aligned} \tag{4.2.7}$$

The determined runoff volume is again distributed over the whole storage, as described previously.

As third parameter an offset analogous to the dead storage concept was introduced on the top of the upper storage, in order to exclude very recent waters from the runoff (and thus reach more effective damping particularly

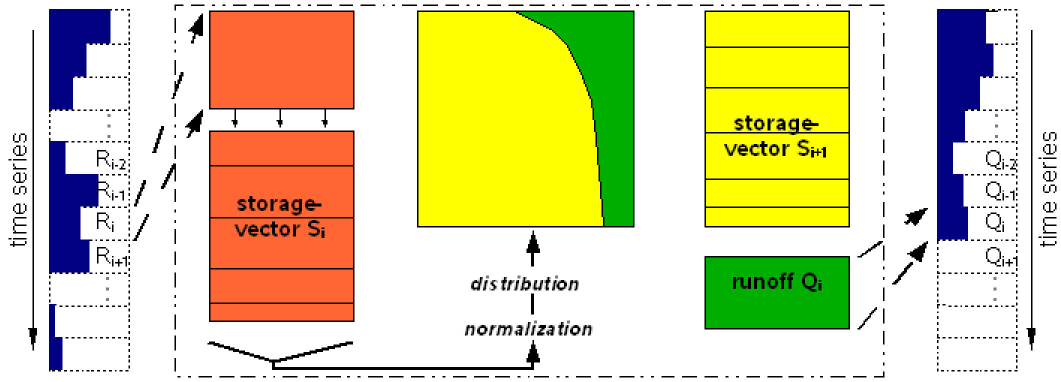

Figure 4.2.4: Modelstructure: Overview of the computations in one time step. Only the volume routine is pictured.

during snow melt). But as it turned out to be not sensitive in the model evaluation it was eventually discarded in the model.

4.2.3 R-coded example

In this section an implementation of the above explained distribution model in one single linear storage is provided, written in the statistical language R (URL1). It is written as a function, which can be applied to vectors of precipitation and precipitation concentration time series. Additionally, the desired runoff and distribution coefficients (κ) have to be passed to it.

This is meant to be exemplarily, in order to keep it simple no dead storage parts are integrated. The code can be copy-pasted to the R Console and is executed with:

```
> linconc([RUNOFF COEFFICIENT],[DISTRIBUTION COEFFICIENT],
+ [PRECIPITATION],[PRECIPITATION CONCENTRATION])
```

The results are merged into a dataframe including in- and output time series.

```
linconc <- function (A, B1, N, CN) {
# A : runoff coefficient
# B1: distribution coefficient
# N : precipitation time series
# CN: precipitation concentration time series
S <- c()        # storage time series, vector (numeric)
Q <- c()        # discharge time series, vector (numeric)
CQ <- c()       # discharge concentration time series, vector (numeric)
SVECend <- c()  # inititialize end-of-time-step-storage vector
CVEC <- c()     # analog for storage concentration vector
for (i in 1:length(N)) {
  ## storage, discharge AMOUNT
  if (N[i]==0 || is.na(N[i])) SVEC<-SVECend
  else SVEC <- c(N[i],SVECend)      # refresh storage vector
  Q <- c(Q,sum(SVEC)*A)      # discharge amount, the single linear store
  SNORM <- (SVEC/sum(SVEC))    # scaling storage vector to a sum of one
  # integration, discharge DISTRIBUTION
```

```
  B2 <- (-B1*A)/(exp(-B1)-1)
  CUM1 <- cumsum(SNORM)
  CUM2 <- c(0,cumsum(SNORM)[-length(SNORM)])
  INTE <- (B2/-B1)*(exp(-B1*CUM1)-exp(-B1*CUM2))
  QVEC <- INTE*sum(SVEC)
  SVEC <- SVEC-QVEC
  # calculate concentration
  if (N[i]==0 || is.na(N[i])) CVEC <- CVEC
  else CVEC <- c(CN[i],CVEC)
  CQ <- c(CQ,sum(CVEC*QVEC)/sum(QVEC))
  # clearing up the storage vector from entries smaller < 0.1 mm,
  # added to the next younger entry
  # starting at a length > 100
  if (length(SVEC)>100) {
   for (i in 2:length(SVEC)) {
    if (SVEC[i]<0.001) {
     CVEC[i-1] <- (CVEC[i-1]*SVEC[i-1]+CVEC[i]*SVEC[i])/(SVEC[i-1]+SVEC[i])
     CVEC[i] <- NA
     SVEC[i-1] <- SVEC[i-1]+SVEC[i]
     SVEC[i] <- NA
    }
   }
  }
  CVEC <- as.numeric(na.omit(CVEC))
  SVECend <- as.numeric(na.omit(SVEC))
  S <- c(S,sum(SVECend))
}
# output
#SFR1<<-data.frame(SVEC,QVEC,INTE)  # storage vector in the last time step 1
#SFR2<<-data.frame(SVECend,CVEC) # storage vector in the last time step 2
TFR<<-data.frame(N,CN,S,Q,CQ) # output time series, dataframe
}
```

4.3 The final HBV-^{18}O model

4.3.1 Modifications and additional parameters

In the preceeding chapter a description of the neccessary manipulations within the HBV's storage structure was given. Thus the HBV code was partly rewritten in order to implement these changes. Figure 4.3.1 shows an overview of the finally used model structure. While the general model design is left unchanged, several internal and interactional modifications were made.

Beginning at the moment that a water amount "enters" the model, not only the actual amount but also the ^{18}O concentration and the age (days) will be transported along. The age is subsequently counted up in the following timesteps and then used to compute mean transit times in the runoff for every timestep.

In case of snow condition the snow storage starts up. Only few alterations were made in this part. Melting water will be composed of every snow part equally, which is Good Mixing. This is of course a weakness, but considering the fact that the snow module is very simple it seems to be legitimate not to put too much effort into it. Melting water or rainfall respectively is then routed to the first storage, possibly diminished by the soil storage.

The evapotranspiration is not further taken into consideration. According to Gat (1996), transpiration fluxes do not produce significant fractionation. And evaporation from soil plays only a minor role in forested catchments.

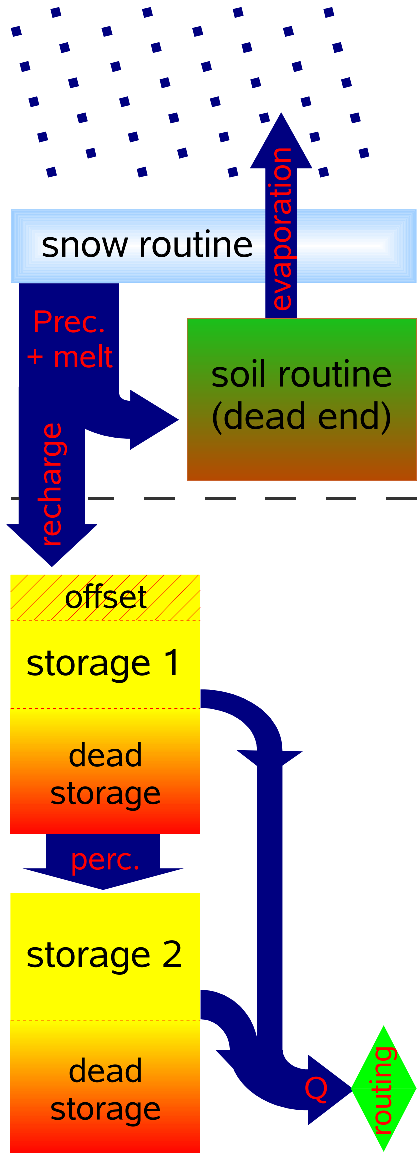

Figure 4.3.1: The modified HBV-^{18}O model, structural overview.

The upper storage, corresponding to fast runoff reactions and "top layer generated" runoff, obtained three new parameters: *ExpParam1* (nondimensional) which triggers the steepness of the distribution curve, *Store1* (mm) the size of the dead storage below the active part and additionally *Offset* (mm) an analogous to the dead storage unactive storage volume on top of the upper storage which however turned out to be very non-sensitive. The lower storage is arranged likewise, with parameters *ExpParam2* and *Store2*. The program menu *Parameter* is shown in the appendix,

Table 4.3.1: Distribution model parameters and model behaviour, overview.

	ExpParam	**Store**
small	Good Mixing runoff	fast turnover, hardly any seasonal damping, small aquifer
large	strong exponential distribution, preferably young runoff	long input memory, strong ^{18}O variation damping, big aquifer

page 61.

The percolation from the upper to the lower storage (controlled by parameter *PERC*, see section 3.1) in the form of Good Mixing percolation from all components of the upper storage (dead and active) only takes place in periods when the upper storage contributes to runoff.

The valid parameter ranges and subsequent storage behaviours are displayed in table 4.3.1. The *Store* parameters range from > 0 to ∞ (actually 1.8E+308, the 'double float' number range). It is important that they have to be non-zero, otherwise the program will crash with a runtime error. Large *Store* values will raise the mean age and are indicated in areas with extensive aquifers. The *ExpParam* parameters have the same lower limit (> 0). Their ranges are capped upwards by the active runoff coefficients *K1* and *K2*. According to equation (4.2.5) in section 4.2.2 the parameters are validated and a warning *"ExpParam out of range"* is prompted to the user if the validation fails. With HBV parameter names the validation formula is:

$$1 \geq -\frac{ExpParam}{e^{-ExpParam-1}} \tag{4.3.1}$$

The closer the *ExpParam* values get to zero, the more the storages' runoff will resemble a Good Mixing runoff. Vice versa if *ExpParam* is large, the distribution curve will be steep and preferentially young water will contribute to runoff.

The timeseries input file `ptq.dat` now contains two further columns cP and cQ, that represent ^{18}O concentrations of precipitation and runoff respectively. Precipitation concentrations currently have to be corrected as described in section 2.2.2 on page 15.

Note that there **must** be a (interpolated) concentration available for every precipitation volume, but not for the runoff. Empty fields are represented by -999. The new input file looks like this example:

```
Brugga Date,P,T,Q,cP,cQ
000101,8.9,0.760447836,5.455356784,-11.395,-999
000102,2.4,-0.439349054,5.175316583,-11.395,-999
000103,0,-2.088809189,4.615236181,-11.395,-999
000104,21.6,2.730869231,4.615236181,-11.395,-999
000105,4.8,2.650467103,6.013266332,-11.395,-999
```

...

The simulated ^{18}O time series is currently not plotted in the model's plot interface. This may be updated in future versions. Instead they can be found in the results file `resuxxx.dat` as the new column cQsim.

Additionally the mean transit times of runoff water is computed from the contributing storage components. These can be found in the results file as well as column ageQsim.

The HBV program slows down drastically with the modifications made, because a lot more information is transported through it (storage heights in form of floating point values have been replaced by storage arrays with several hundred elements on which calculations in each timesteps are performed). The advised order to fit a catchment is to do the quantitative fit in the original HBV model and subsequently take the resulting parameter set and fit the transit time model in the modified version. The distribution model has to fitted by trial and error. Note that the Warm up period, in which the model approaches steady state conditions can prolong drastically, depending on the volume of the dead storages.

4.3.2 Model behaviour: artificial datasets

The modified HBV model finally incorporates the possibility to store reasonable amounts of water inside the model catchment and to pass storage components in an exponential-shaped distribution onto the runoff while the quantitative HBV routine is kept unaffected.

In order to illustrate the behaviour of the model and the reaction in runoff δ^{18}O concentration on different parametersets two artificial datasets were created. One showing a constant precipitation input with also constant δ^{18}O concentrations and one a quantitative and qualitative Dirac impulse, the second with constant precipitation and idealized sine-wave shaped δ^{18}O concentration changes along the seasons, as found in the investigated catchment.

All other input variables such as potential evapotranspiration and temperature were assumed to be homogenous, in order to focus on the behaviour of the storages. Further model result time series on parameter variations can be found in the following chapter 5 where model reactions on more complex catchment situations (the actual catchment data) are illustrated. The following sections will just demonstrate the general behaviour of the model.

4.3.2.1 Impulse response

In Figure 4.3.2 and 4.3.3 the model's reaction on a quantitative and qualitative impulse input is displayed. The upper shows variations of the *Store* parameters and their influence on the concentration in the runoff and the lower shows the influence of *ExpParam* variations respectively.

Store1 and *Store2* remained equally-sized with the variation in Figure 4.3.2, but the more important part here is the lower storage as it contributes constantly to runoff whereas the upper only is filled periodically. While *Store* was

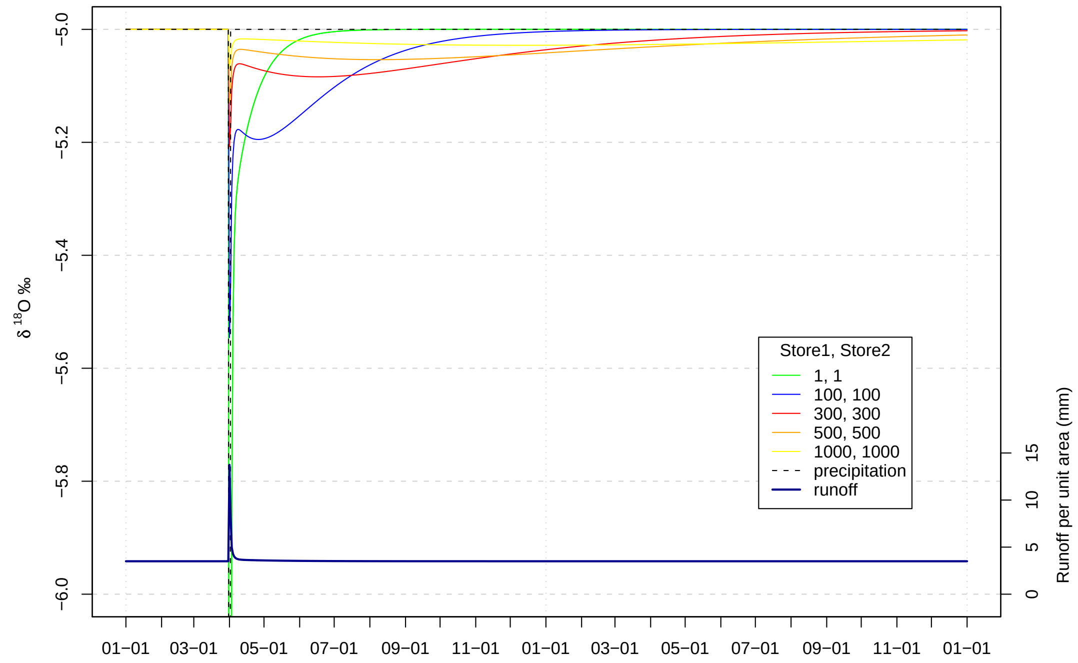

Figure 4.3.2: Variation of "Store" parameters, "ExpParam" parameters fix at 0.01. Further explanations see text.

varied, *ExpParam* (for upper and lower storage) was kept at 0.01, i.e. Good Mixing. The abscissa displays (fictive) time with first-of-month labels. One can see that unless the actual runoff reaction last only for a few days the isotopic fingerprint still can be identified after months very clearly. With growing dead storage volumes the isotopic response function changes from exponentially shaped to a shape that can be described as a shift with nearly constant higher concentration afterwards. This is caused by the lower contribution of the higher concentrated impulse volume in case of bigger dead storages and subsequent slower diminishment of the contributed amount.

A second effect which can be seen in the time series is the bow the curves describe after the first recession of the concentration. This is an effect of the delay as the impulse is passed to the lower storage. The smaller the upper dead storage is, the faster the impulse-transfer to the lower will get.

In Figure 4.3.3 *Store* parameters are fixed at 300 mm and *ExpParam1/2* vary. Though the example displays a rather small aquifer volume the effect of an increasingly exponential runoff distribution can be seen. While under small *ExpParam* values the impulse shows the previously described shift, with increasing *ExpParams* the younger storage parts gain more and more weight and consequential the "bleaching" velocity increases. The last, yellow graph shows the effect of a Good Mixing upper and exponential lower storage. The impulse is delayed due to the upper storage behaviour and decreases exponentially and relatively fast due to the lower.

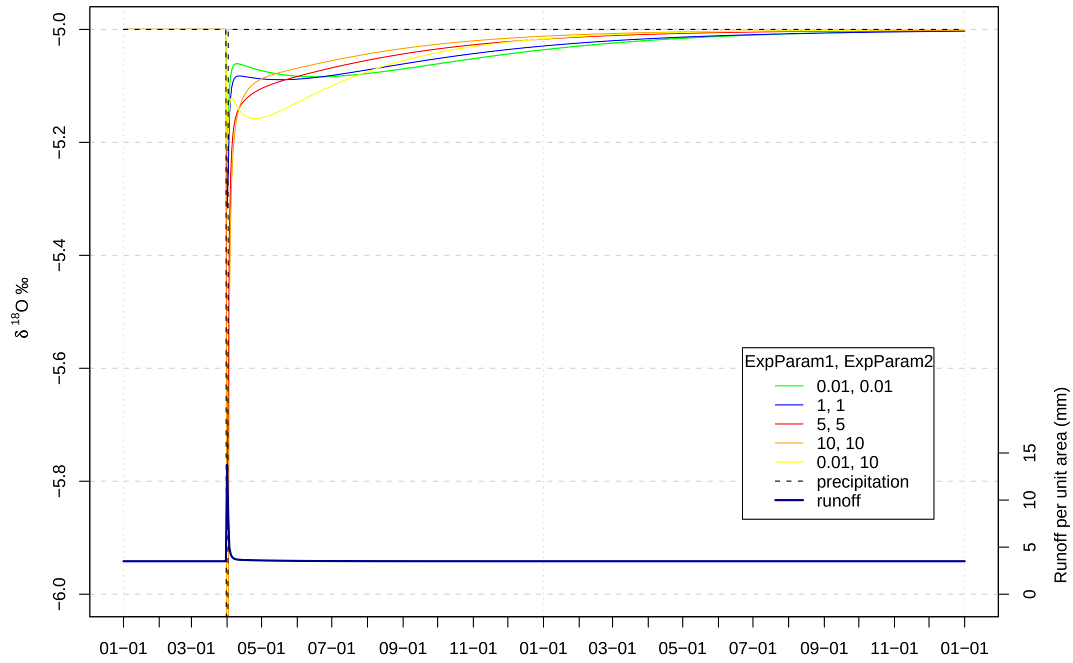

Figure 4.3.3: Variation of "ExpParam" parameters, "Store" parameters fix at 300 mm. Further explanations see text.

4.3.2.2 Sine-wave response

As an example of the model's reaction to a more realistic input time series a sine-wave shaped artificial $\delta^{18}O$ concentration time series was passed to the model. The precipitation volumes however were kept constant ($5\ mm/day$). Figure 4.3.4 and 4.3.5 show the effects of parameter variation analogously to the previous two figures. Apparently the model is capable to reproduce the most obvious effect of input tranformation; the response function shows distinct damping compared to the input function.

The increasing dead storages (with Good Mixing distribution) in Figure 4.3.4 evoke an increasing damping and phase lag in the response time series.

When the distribution function is changed towards a more exponential shape (increasing *ExpParam*, see Figure 4.3.5), the damping is partially reversed. Additionally though, and this is not visible in the example due to the uniform sinus function, older volumes in the storage will remain longer in the storage than with Good Mixing distributed runoff and thus in times of low runoff the model is more likely to return a longterm mean of input concentrations (in case the overall size of the storage is sufficiently big, of course). I.e. a 2-year sinusoidal input time series with two different amplitudes will result in a more homogenous response series amplitude when the *ExpParam* values are high.

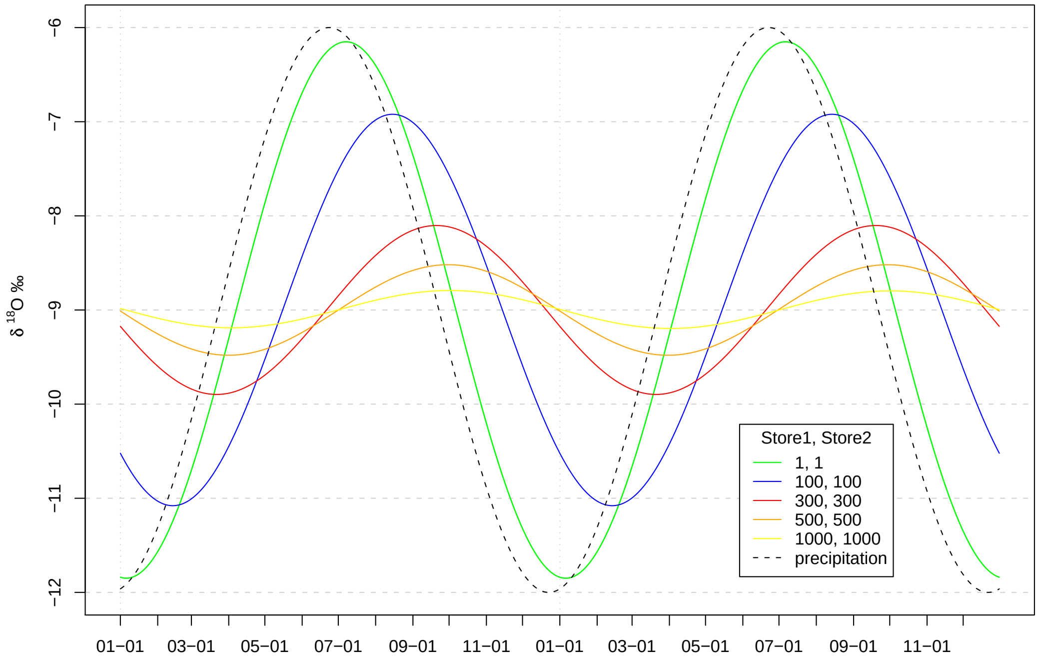

Figure 4.3.4: Variation of "Store" parameters, "ExpParam" parameters fix at 0.01. Further explanations see text.

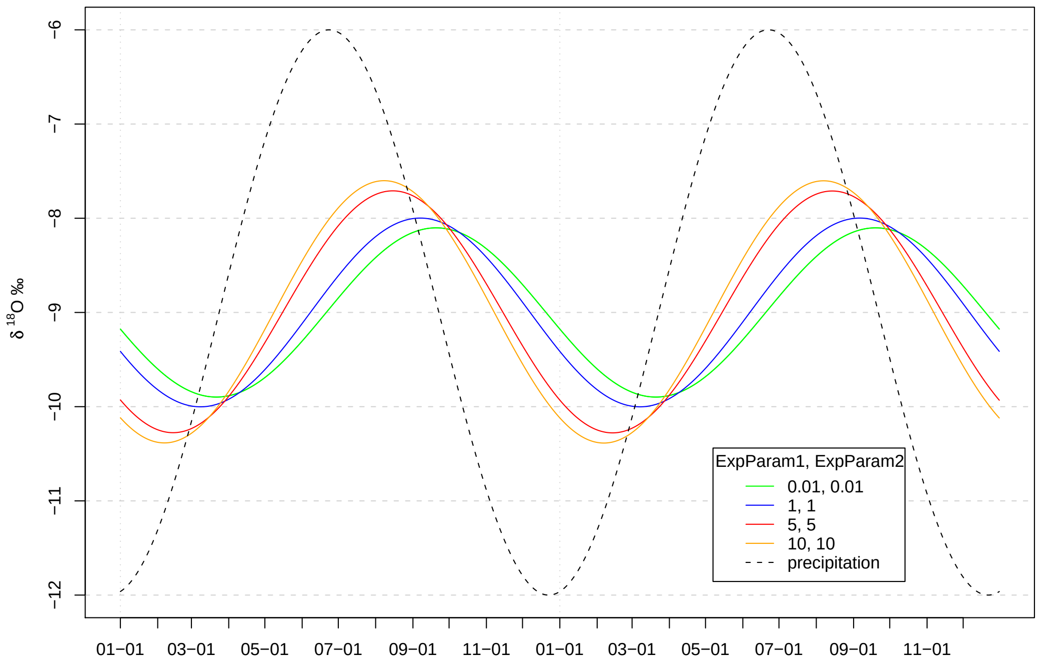

Figure 4.3.5: Variation of "ExpParam" parameters, "Store" parameters fix 300 mm. Further explanations see text.

4.4 Conclusions

The HBV model had to be altered in order to be capable of computing $\delta^{18}O$ transport in a catchment scale. A conceptual approach to integrate a distribution model into the existing model's single linear storage structure had to be formulated. This was done under consideration of pathway distribution which would lead to the assumption of an exponential transit time distribution in the investigated mountainous catchments. A versatile, Good Mixing to exponential shaped adjustable and low parametrized (two additional parameters per storage) distribution approach was then successfully implemented into the HBV model.

Other, probably important, effects such as snow fractionation had to be neglected though.

5 HBV-^{18}O: Results & discussion

5.1 Brugga

The Brugga section comprises the major part of this Chapter. It includes, besides the results of the model application in the catchment, a couple of figures with parameter variations in order to show the model behaviour and parameter sensitivity under realistic conditions as well as a description of necessary input time series preparations. Specific attention will then be paid to the development of stream water transit times, especially during drought conditions and an interpretation of the underlying hydrological processes.

5.1.1 Time series description and runoff simulation

Figure 5.1.1 gives an overview over the input time series of δ^{18}O concentration in precipition and runoff as well as specific runoff and precipitation amounts (indicated by point sizes of precipitation-δ^{18}O). The runoff responds fast and volatile to precipitation events, as well in winter- and springtime with generally higher runoff as during midflow conditions. The δ^{18}O concentration in precipitation shows a strong seasonal variation with an approximate mean amplitude of 15 ‰.

Despite the runoff's volatility and the strong variability in δ^{18}O input, the δ^{18}O concentration in runoff varies little, especially not significantly during storm runoff when a high contribution of event water would be expected. It rather seems to be constant compared to precipitation. However although the δ^{18}O response is strongly damped and also lagged it still shows a significant seasonal variation with a nonetheless a lot smaller amplitude than δ^{18}O in precipitation (see also the figures in chapter 6).

The heaviest precipitation in the investigated period was measured during the extraordinarily hot and dry summer saison 2003. Remarkably, this is also a period with a distinct trend in runoff δ^{18}O (towards a higher concentration).

The first modelling step was to fit the quantitative model in order to create the transit time model "environment" as described in the previous chapter. The simulated runoff, along with measured precipitation and runoff, can be seen in Figure 5.1.2. The appendant R_{eff} is 0.81. Overall, the simulated values fit the measured ones quite well, although not every runoff peak is covered perfectly and especially in phases when runoff declines the simulated values seem to overestimate runoff a little bit. But under consideration of e.g.

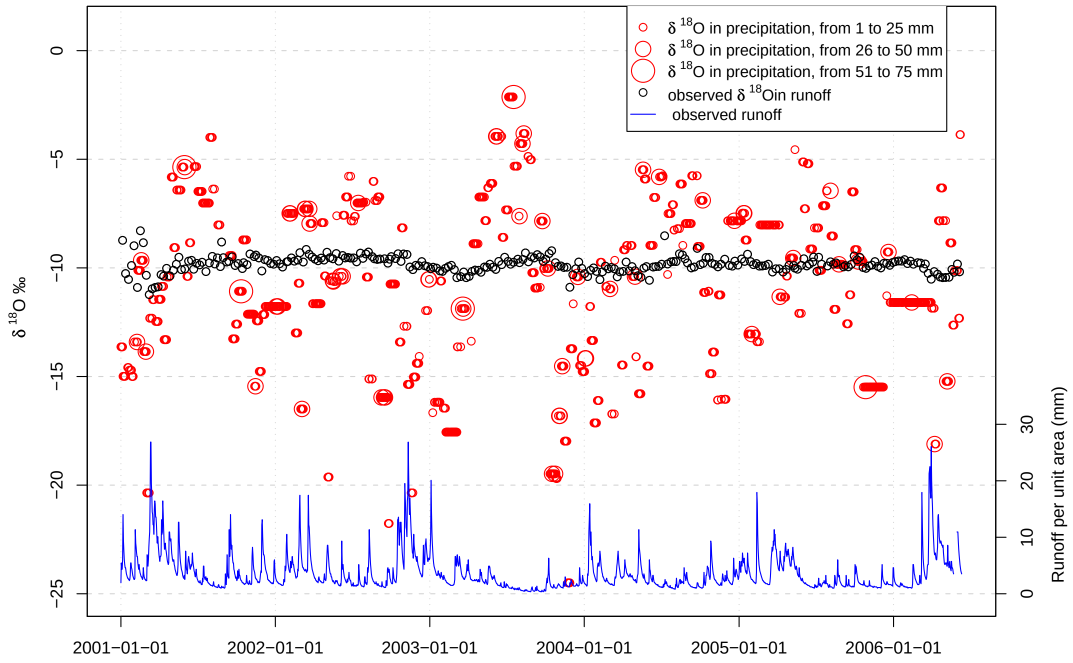

Figure 5.1.1: Brugga catchment, time series of specific runoff (mm), δ^{18}O concentrations in precipitation and runoff. The size of precipitation concentration points depends on a volume ranking (volume classes in the legend).

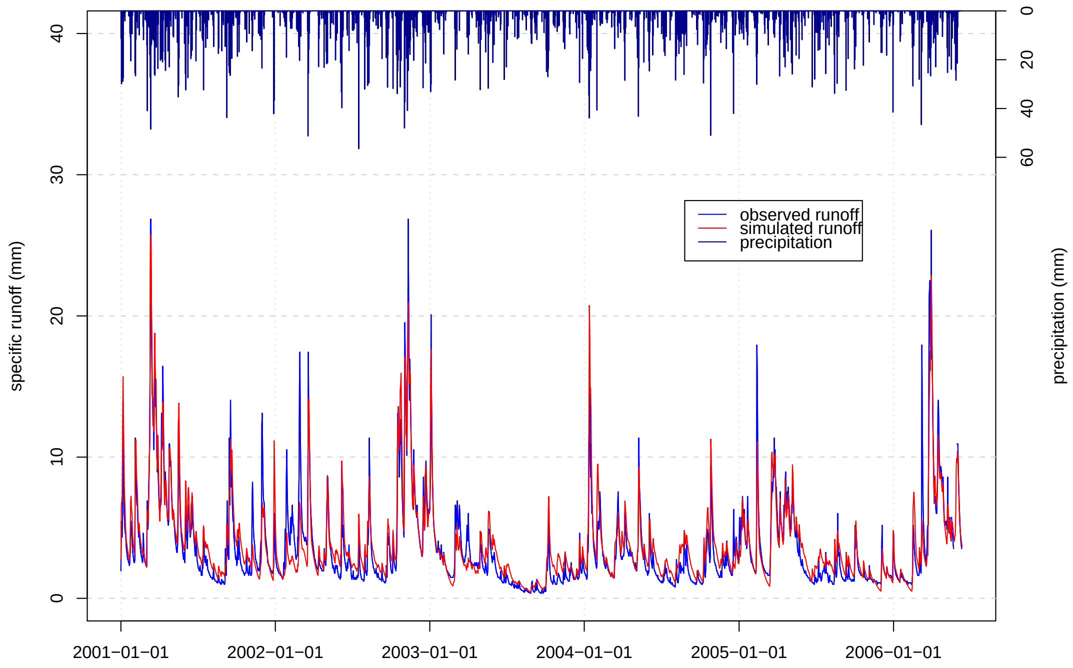

Figure 5.1.2: Precipitation, observed and simulated runoff in the Brugga catchment.

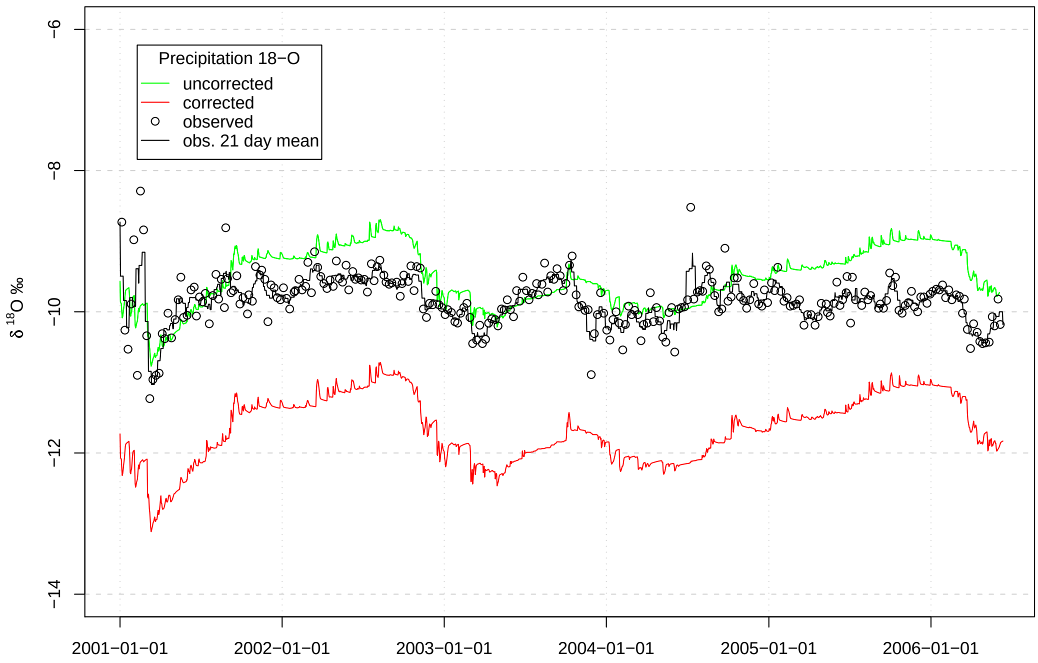

Figure 5.1.3: Exemplary model run with corrected and station-measured δ^{18}O input in the Brugga catchment.

uncertainties in precipitation measurements, particularly in wintertime when it comes to snow, or general interpolation uncertainties (point-area, gradients with elevation), this model fit is probably as good as it can get.

The model was set up with eleven elevation zones of 100 m extent with three landuse zones each. The respective landcover- and elevation-distributions were taken from Holocher (1997). Complete parameter sets can be found in the Appendix (Table A.1, A.2).

5.1.2 Input- and steady state issues, parameter variations

In Section 2.2.2, a correction of the measured δ^{18}O precipitation time series was proposed because an altitude dependency caused by the height effect was assumed in the mountainous catchments. Looking at Figure 5.1.3, this assumption was obviously wrong. The red curve is the corrected input and lies clearly and systematically below the measured concentrations while the green curve shows largely congruence with the measured values. This fact will be adressed further in the next section.

In a first approach the time series were passed to the model without further manipulation and a warm-up period of one year. The result of such a model run can be seen in Figure 5.1.4. The red and blue lines display measured and simulated specific runoff (mm), black and green are the appendant δ^{18}O concentrations.

The transit time model parameters have values of: 1000, *Store1*; 1500,

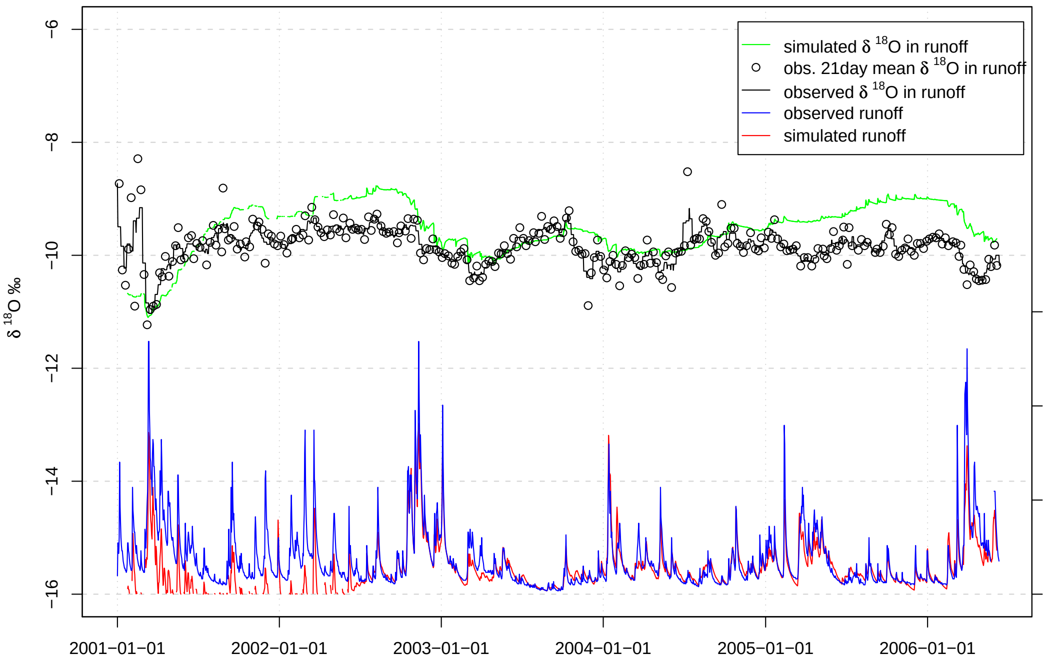

Figure 5.1.4: Model run with one year warm-up period, observed and simulated runoff differ due to the unfilled storages, Brugga catchment.

Store2; 0.01, *ExpParam1*; 16, *ExpParam2*. In total 2500 mm dead storage have to be filled, untill the model starts approaching steady state. With one year warm-up this cannot be achieved (mean yearly precipitation over the investigation period: 1418 mm). In 2001 and 2002 the modelled runoff is far below the measured and even falls dry because the lower storage is not filled sufficiently yet. The δ^{18}O curve appears to be dashed in that period because zero values during dry phases have been omitted in the plot. Additionally, in the beginning the modelled aquifer consists only of water from the year 2000 which can disturb the simulation e.g. in case a longterm mean is present in the lower storage.

Therefore, and so that the longest possible time series could be modelled the years 2000 to 2005 were duplicated and passed twice to the model. Thus the storage components were best possible filled and preset in the beginning of the actual simulation period in 2001.

The in such a way prepared input data were subsequently fitted to the measured data as good as possible. In order to illustrate the parameter sensivity a couple of model runs with different parameter sets will be shown.

The variation of the runoff-distribution parameter *ExpParam*, shown in Figure 5.1.5 with fix values of 1000/1500 mm for *Store1*/*Store2*, influences the portion of young water in runoff. With higher values of *ExpParam* and following higher portion of young event water the response curve scatters, especially during flood periods, i.e. winter saison. The upper storage with *ExpParam1*

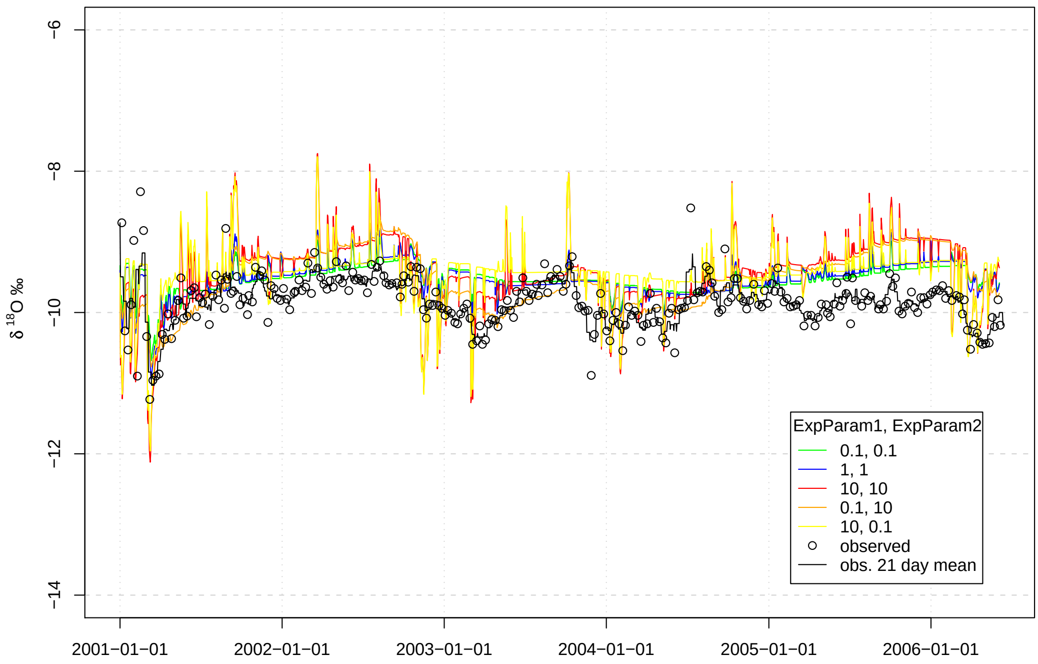

Figure 5.1.5: Variation of parameter *ExpParam* in the Brugga catchment.

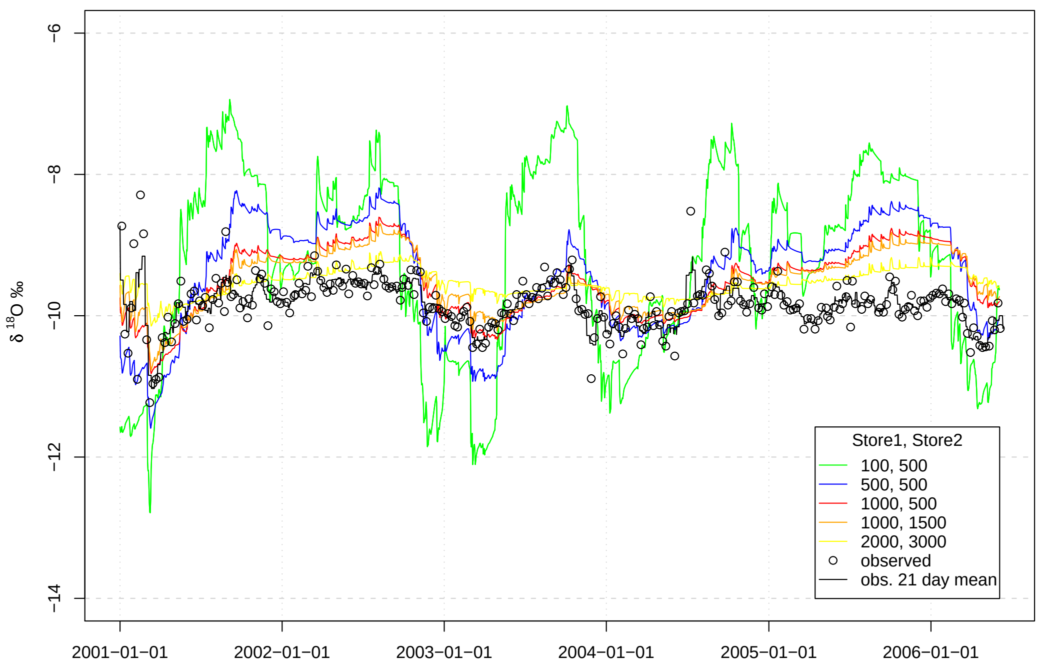

Figure 5.1.6: Variation of parameter *Store* in the Brugga catchment.

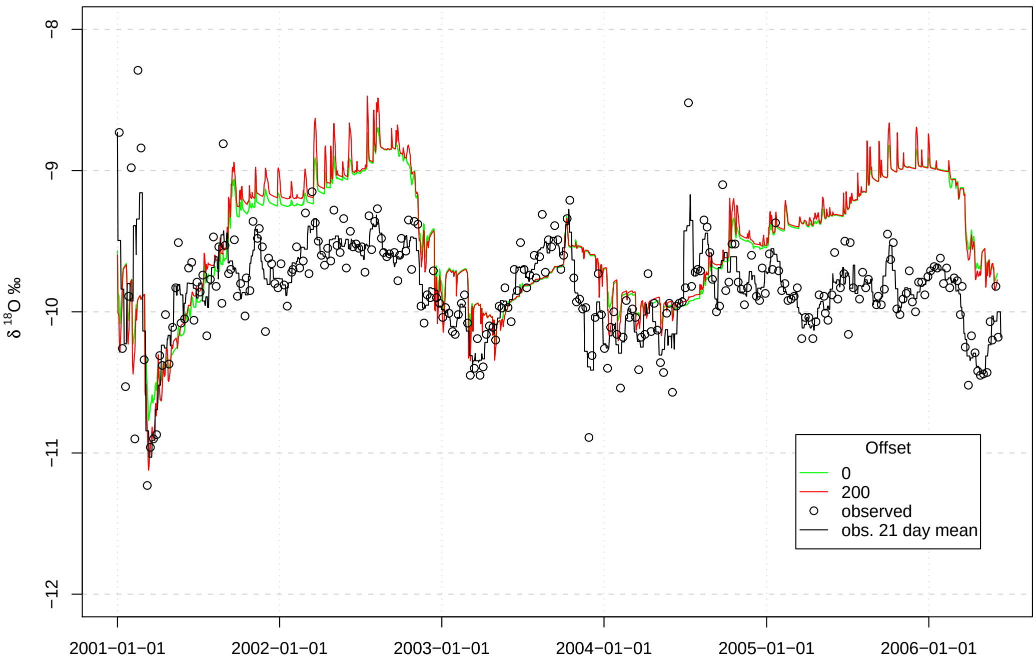

Figure 5.1.7: Variation of parameter *Offset* in the Brugga catchment.

tends to be more sensitive to scattering because it receives pure event water whereas the lower storage receives mixed water (see yellow curve). The lower storage with *ExpParam2* influences the annual curvature first.

5.1.3 HBV-^{18}O model fit and transit time development

For the Brugga catchment, the model was finally parametrized with these parameter values: 1000, *Store1*; 1500, *Store2*; 0.1, *ExpParam1*; 10, *ExpParam2*. The result is shown in Figure 5.1.8. Generally, the simulated δ^{18}O in runoff (green) fits quite well to the measured values.

Nonetheless, particular in 2002 and 2005, the model develops an offset towards heavier δ^{18}O concentration. Two possible explanations can be considered. Either the model has a conceptual deficit that evokes a drift toward heavier values, e.g. the recharge might be distributed differently throughout the year than the model-computed is, and higher isotope enriched water than in reality enters the storage system. Or that effect is caused by an incorrect input function, i.e. the precipitation concentration which is not corrected in any way. Table 5.1.1 summarizes a couple of mean, maximum, and minimum values. Looking at the overall means of precipitation and runoff δ^{18}O, the value for precipitation (-9.147 ‰) is about 0.8 ‰ heavier than the mean of measured runoff Q_m (-9.939 ‰) whereas the value for simulated runoff Q_s (-9.593 ‰) is closer to precipitation (the difference is probably caused by the water stored in the model at the end of the simulation period and warm up

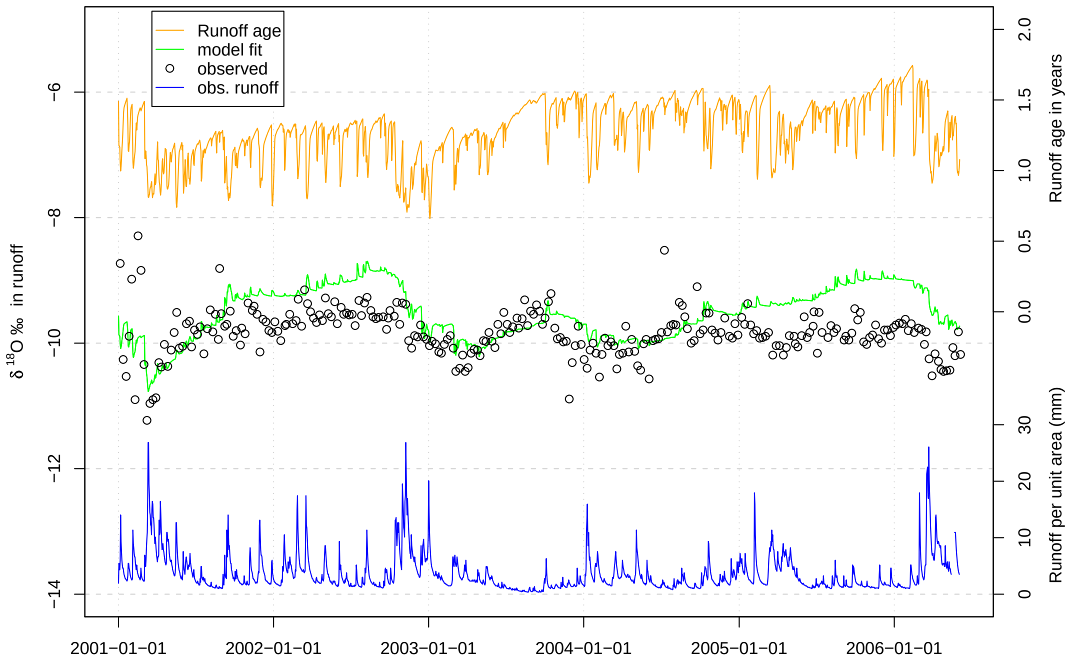

Figure 5.1.8: Final transit time fit with transit time development (runoff age), measured and modelled δ^{18}O in runoff as well as measured specific runoff, Brugga catchment.

Table 5.1.1: Modeled transit time results (age, in years) and δ^{18}O time series means (volume weighted), Brugga catchment

	Mean age Q	Min age Q	Max age Q	Mean ^{18}O P	Mean ^{18}O Q_m	Mean ^{18}O Q_s
overall	1.3	0.7	1.7	-9.147	-9.939	-9.593
2001 – 2002	1.1	0.7	1.5	-9.266	-9.863	-9.598
2003	1.3	0.7	1.6	-8.938	-10.022	-9.818
2004 – 2006	1.4	0.9	1.7	-9.081	-10.005	-9.523

period-contributed water, a small part could also be explained with roundoff errors). However, the deviation is both small and not distributed uniformly over the simulated period. Thus, a general altitude dependency cannot be confirmed.

The simulated transit time, plotted orange in Figure 5.1.8, reveals three major characteristics of transit time development throughout the investigation period. If the simulation is trustworthy, storm events reduce the mean transit time of stream water substancially but shortly (up to a mean transit time reduction of 0.5 years), this happens without leaving a distinct fingerprint in the δ^{18}O composition of stream water. Furthermore, no regular periodical oscillation throughout the seasons can be found, unless there are phases of medium-term changes that overlie the short-time collapses.

The most important observation regarding the objective of this thesis is

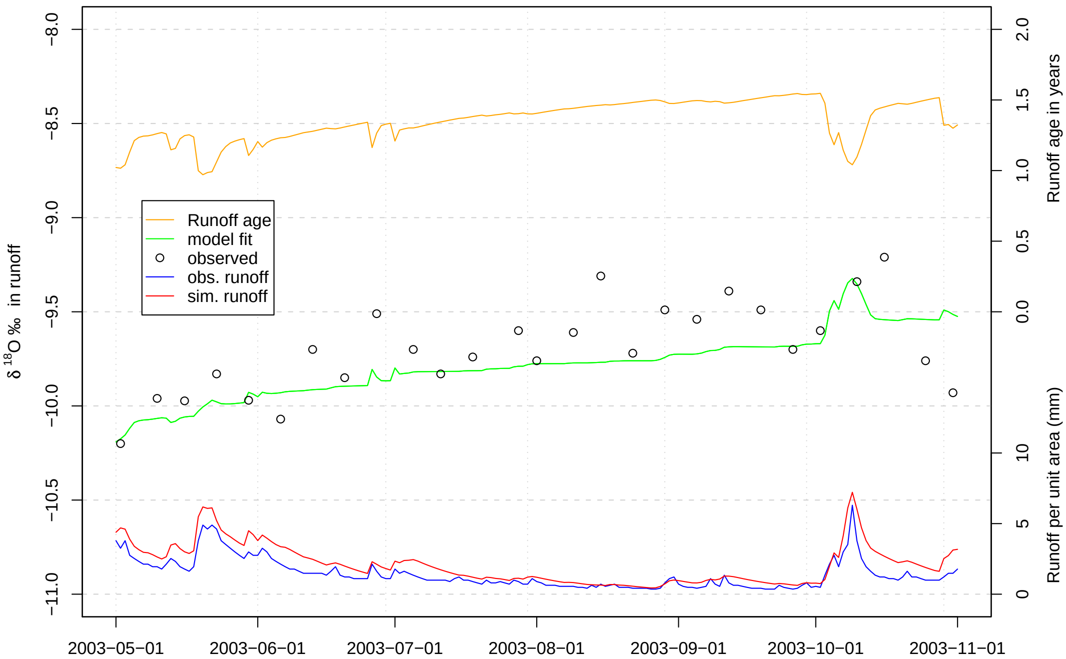

Figure 5.1.9: Transit time development during the dry spring/summer in 2003, Brugga catchment.

the shift towards higher mean transit times in connection with the warm and widely snowless winter season 2002 – 2003 and the following hot and dry summer season 2003. Due to the low snow accumulation and enduring stormflow conditions, the mean transit times in streamwater show a decline of about three months in November/December 2002. Subsequent to the warm winter, the stream water age starts to rise up to about 1.5 years which is also reflected in the isotopic streamwater composition (see Figure 5.1.9). This process is summarized in the raise of mean transit times for the pre-drought period 2001 – 2002 of 1.1 years to a post-drought level of 1.4 years (2004 – 2006, see Table 5.1.1). Maybe the change starts to recede with the beginning of 2006, but at least until then the drought is still detectable in the transit time signal. That is, the catchment has still not recovered from the 2003 drought.

Figure 5.1.10 displays the probability mass function (PMF) alongside with the cumulative distribution function (CDF) of the simulated transit time. Quartiles are displayed by the x-axis tick marks. The PMF shows two distinct peaks which refer to the pre- and post drought conditions. The CDF is S-shaped with a steep quasi-linear character between first and third quartile. Only 17 % of the age distribution is covered by 50 % of the simulated transit time values. This reflects the overall homogeneity of stream water ages in combination with the short collapses during storm events.

As the concentration model currently has to be fitted manually, a certain bias results from the validation or rejection of similar simulation results. In

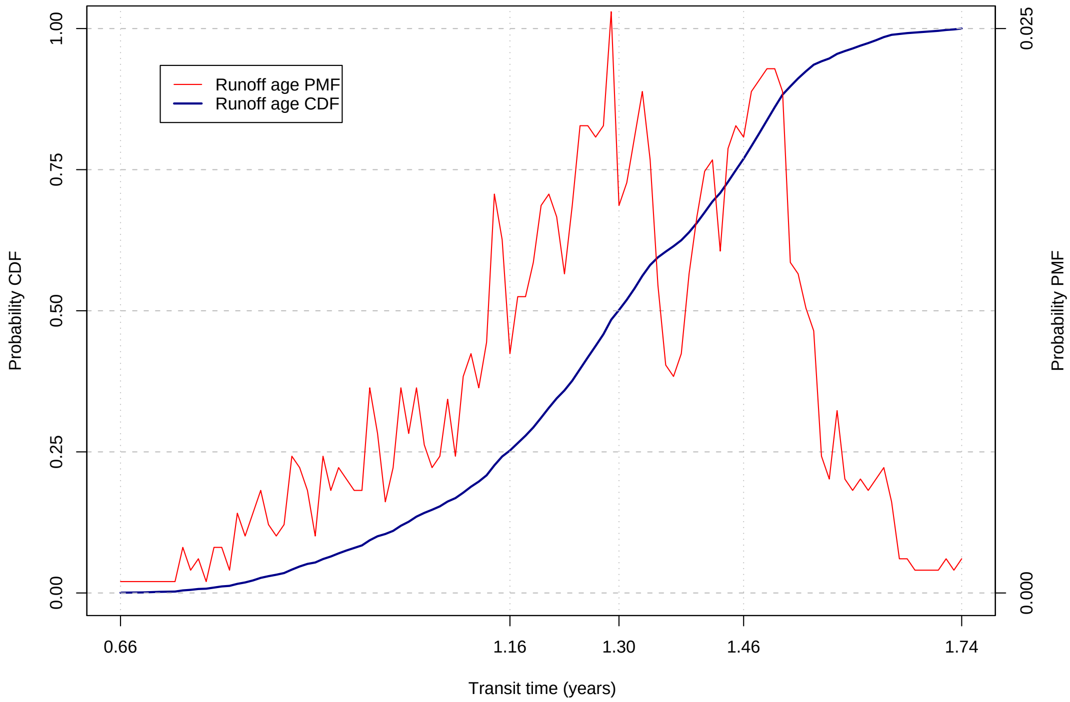

Figure 5.1.10: Transit time in the investigated period: probability mass function (PMF) and cumulative distribution function (CDF), Brugga catchment.

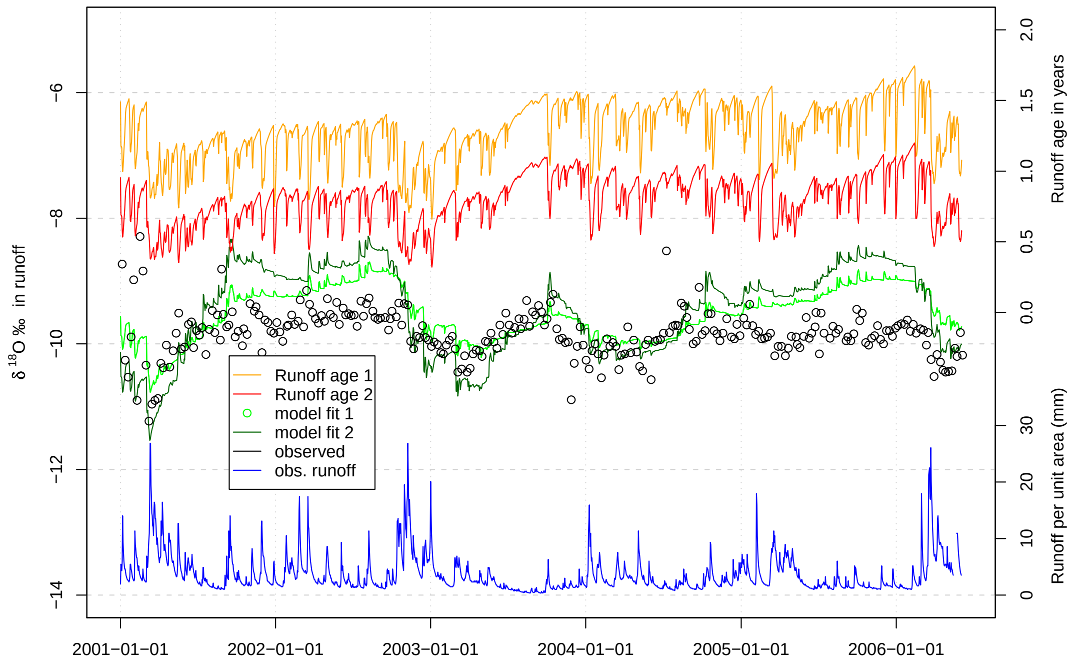

Figure 5.1.11: Comparison of the transit time development in relation to parameter variation, Brugga catchment.

order to depict the reaction of simulated transit time on different parameter sets, two model fits and the appendant transit time series are plotted in Figure 5.1.10. Model fit 1 (light-green curve) is the finally used simulation, whereas for model fit 2 (dark-green curve) the following parameters were used: 500, *Store1*; 1000, *Store2*; 0.1, *ExpParam1*; 10, *ExpParam2*. The dead storages contain 1000 mm less water compared to the final parametrization. That is reflected in the higher seasonal fluctuation of the runoff δ^{18}O concentration and reduces the mean stream water transit times by approximately 0.5 years. The short-term reactions in contrast remain unaltered because the *ExpParam* values were not changed.

Thus, there can be a relevant alteration of the transit time development, caused by changes in the parametrization that result only in minor changes is the simulated δ^{18}O time series and the decision to accept or discard a model run has to be decided with care. Furthermore, one has to keep in mind that the resulting transit times always bear a considerable uncertainty even if the model in general is accepted being reliable.

5.1.4 Conclusions

The newly implemented model parts have been tested successfully. It was possible to reproduce the damping and phase lag from precipitation to runoff δ^{18}O with the Brugga time series. A height correction of δ^{18}O turned out to be unuseful, at least in the form of a constant gradient. A mean transit time of 1.3 years was calculated from the model results over the whole simulation period in the Brugga catchment. Additionally, a shift in mean transit times was detected, developing from the drought conditions in 2003. The mean transit time before the drought results in 1.1 years, 1.4 years were calculated after the drought from the daily time series.

Although the results seem to be hydrologically reasonable, they have to be interpreted with caution because the uncertainties of the simulation as well as possibly wrong assumptions in the conceptual model structure can lead to incorrect conclusions.

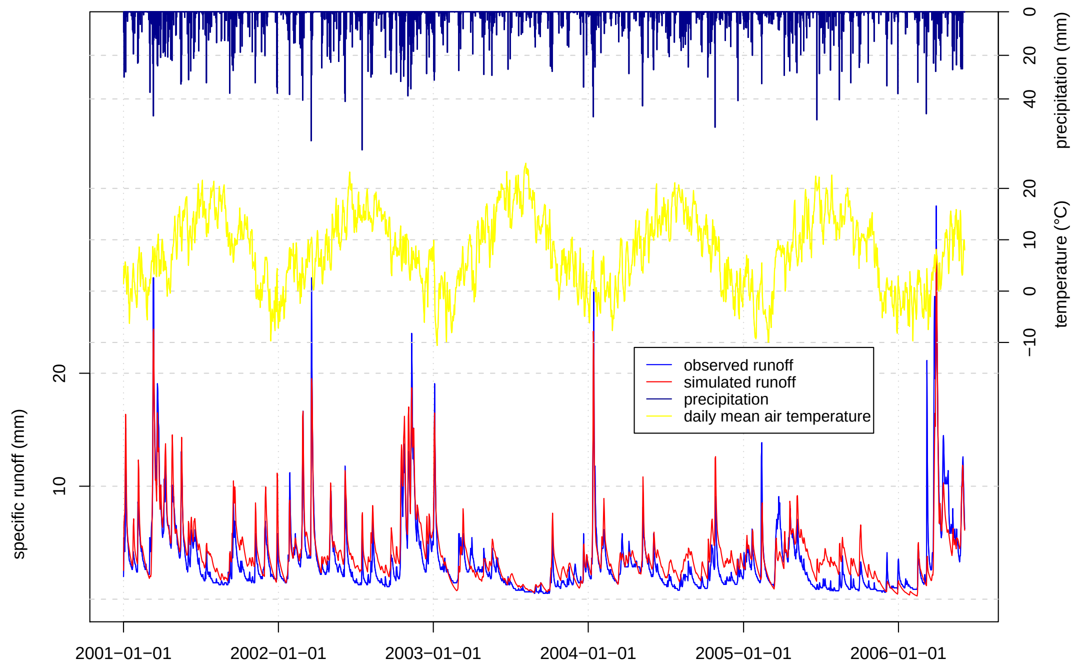

Figure 5.2.1: Precipitation, air temperature, and observed and simulated runoff in the Zastlerbach catchment.

5.2 Zastlerbach

The HBV-^{18}O model was applied analogously in the Zastlerbach catchment, which is smaller than the Brugga catchment but geomorphologically similar. The discussion will be rather short because the results are similar to the Brugga catchment.

5.2.1 HBV-^{18}O model fit and transit time development

Due to the fact that Brugga and Zastlerbach are adjacent catchments the input time series of precipitation look quite similar (Figure 5.2.1). Nonetheless, the runoff peaks in the Zastler time series are steeper and more extreme compared to the mid-flow runoff. This reflects the smaller catchment size with fast runoff concentration and the fast recession after storm events.

The simulated runoff tends to overestimate the measured runoff, especially in the case of smaller storm events that do not yield the intense peaks of bigger events. The model fit is a trade-off between an accurate reproduction of the intensive winter-season peaks and an adequate recession to mid-flow after smaller runoff peaks. The Nash-Sutcliffe efficency R_{eff} has a value of 0.77.

Although this is not a very satisfactory result and increases the overall model-uncertainty, the transit time model has been applied. The time series of measured and simulated δ^{18}O in runoff are displayed in Figure 5.2.2. There is no clear visible difference between the Brugga and Zastlerbach runoff

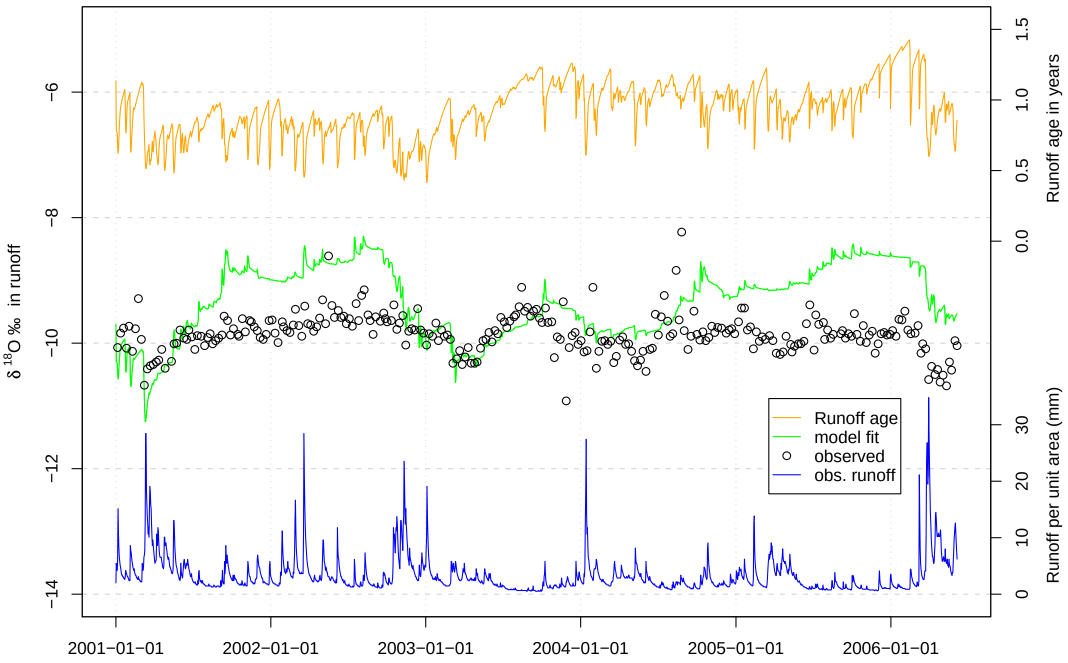

Figure 5.2.2: Final transit time fit with transit time development (runoff age), measured and modelled δ^{18}O in runoff as well as measured specific runoff, Zastlerbach catchment.

Table 5.2.1: Modelled transit time results (age, in years) and δ^{18}O time series means (volume weighted), Zastlerbach catchment

	Mean age Q	Min age Q	Max age Q	Mean ^{18}O P	Mean ^{18}O Q_m	Mean ^{18}O Q_s
overall	0.9	0.4	1.4	-9.113	-9.948	-9.412
2001 – 2002	0.8	0.4	1.1	-9.228	-9.855	-9.422
2003	1.0	0.4	1.3	-8.932	-9.950	-9.856
2004 – 2006	1.0	0.6	1.4	-9.038	-10.055	-9.274

δ^{18}O time series. The precipitation δ^{18}O concentration is exactly the same (combination of both meteorological stations). Accordingly, the fitted simulation is similarily parametrized: 800, *Store1*; 1300, *Store2*; 1, *ExpParam1*; 16, *ExpParam2*. The dead storages have to be smaller than in the Brugga catchment, however, otherwise the simulated runoff concentration time series flattens and does not match the measured variation anymore with the given quantitative model calibration.

The smaller storage volumes result in shorter mean transit times. The overall simulated mean transit time amounts to 0.9 years with a pre-drought estimation of 0.8 years (2001 – 2002) and 1.0 years afterwards (2004 – 2006). Looking at the development in 2003 (Figure 5.2.3), the raise in mean transit time is approximately the same as in the Brugga catchment (0.3 years). But unlike the Brugga, the simulated ages seem to recover in the Zastlerbach catchment

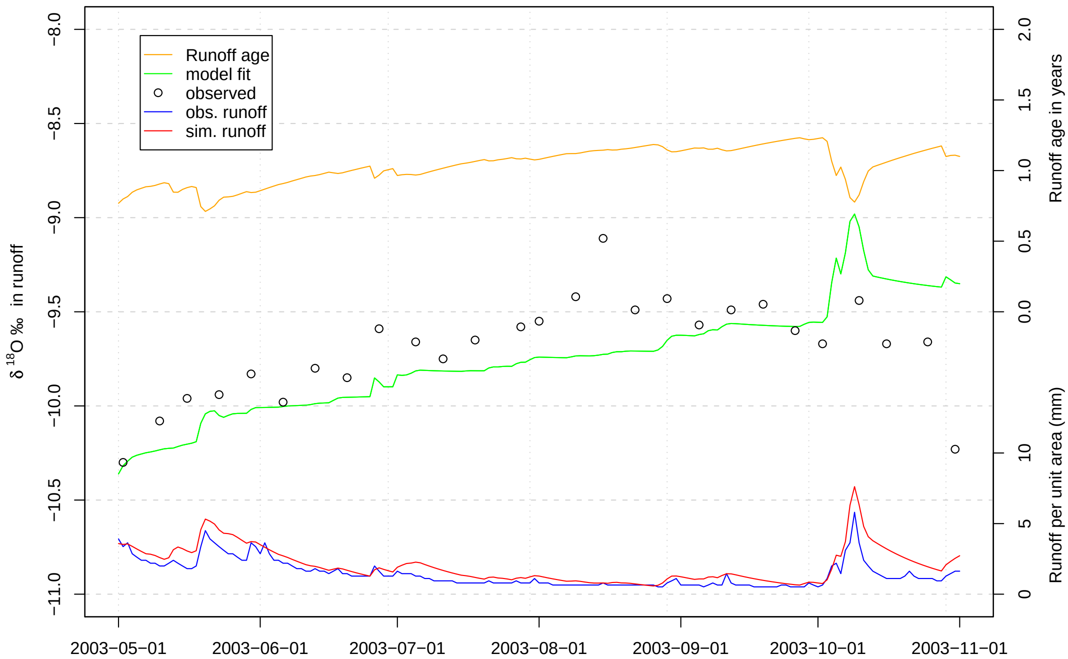

Figure 5.2.3: Transit time development during the dry spring/summer in 2003, Zastlerbach catchment.

from 2003 to 2005.

The probability mass function in Figure 5.2.4 consequently does not show the two peaks as distinct as in the Brugga catchment, the drought effect is already receding.

5.2.2 Conclusions

The simulated mean transit time over the investigated period in the Zastlerbach catchment is 0.9 years. The simulation bears strong resemblance with the adjacent Brugga catchment but in a somewhat alleviated form. I.e., the modelled drought influence is not as long-lasting as in the Brugga catchment and the general catchment behaviour (e.g. runoff reaction) reveals the scale difference between both catchments.

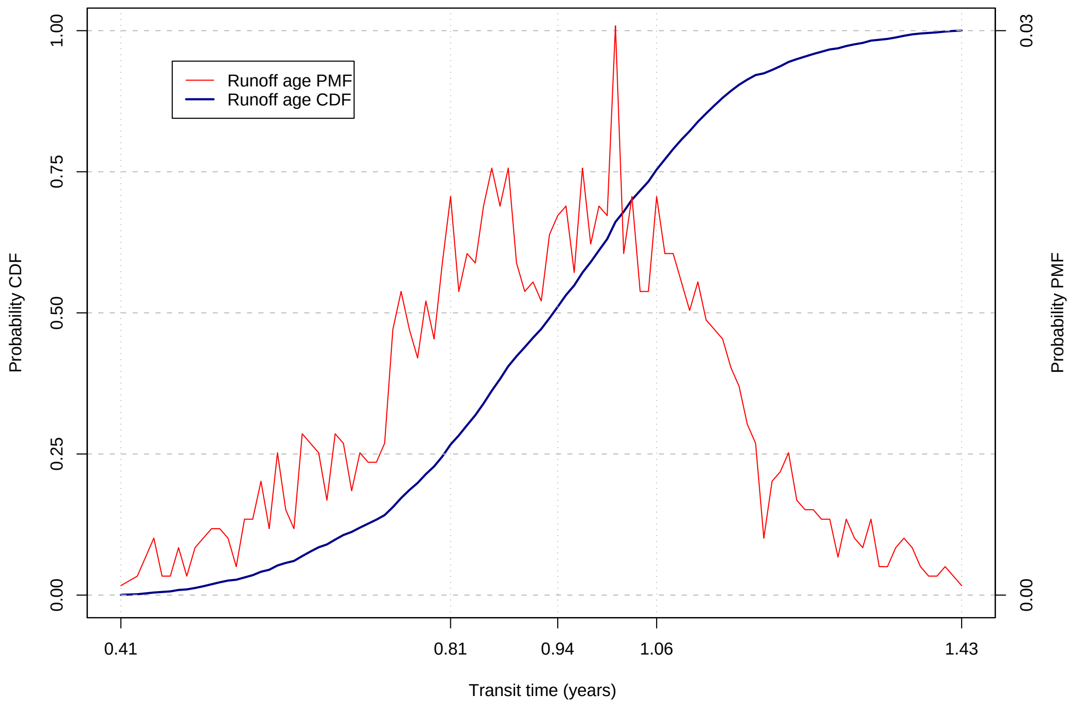

Figure 5.2.4: Transit time in the investigated period: probability mass function (PMF) and cumulative distribution function (CDF), Zastlerbach catchment.

6 Sine-wave approach

6.1 Introduction

For evaluation reasons and in order to get a comparable result with a commonly adapted method, mean transit time estimations were determined by a sine-wave function, representing periodical oscillations in precipitation input and streamflow output concentrations. The application of this method is restricted to areas, where the precipitation shows a reasonable sinusoidal distribution throughout the year (McGuire and McDonnell, 2006). The method is comparatively simple and does not reflect seasonal variations in recharge in the version applied here. Nonetheless, it has been reported to provide reasonable estimations of mean residence times (e.g. DeWalle et al. 1997, Soulsby et al. 2000, Rodgers et al. 2005, McGuire and McDonnell 2006) especially in terms of a potential maximum value for catchment mean transit time, and thus itcan be used for validation of the results presented above. Moreover, since the methodology has been widely applied in residence time investigations, it also provides the possiblity to compare the Brugga and Zastlerbach catchment with other studied sites.

6.2 Method

The sine-wave analysis is a regression statistically evaluating the in- and output time series of $\delta^{18}O$ concentrations (here: precipitation and stream water). Due to fractionation and selection effects (see section 1.3.1, page 2), the $\delta^{18}O$ concentrations often show a significant seasonal variation, which can be expressed with a sine-wave function. Bliss (1970) (in McGuire and McDonnell, 2006) provided a multiple linear regression model to evaluate a sine wave function statistically. Analytical solutions for the mean transit time of the exponential model (EM) and also for the exponential-piston flow model (EPM) exist. Of course, this is limited to locations where precipitation shows a reasonable periodical variation, and damping throughout the flow system does not level the signal completely (which would result in a constant concentration, the mean value of the input function).

The sine-wave function that approximates $\delta^{18}O$ concentrations (δ) throughout the year has the form:

$$\delta = \beta_0 + A \cdot (\cos(ct - \phi)) \tag{6.2.1}$$

with the mean annual stable isotope concentration β_0 (‰), the amplitude A (‰), the phase lag ϕ (rad) and the angular frequency constant c ($2\pi/365$, where t are days) in (rad/d). The parameters in equation (6.2.1) are then evaluated with the regression model.

$$\delta = \beta_0 + \beta_{cos} \cdot \cos(ct) + \beta_{sin} \cdot \sin(ct) \qquad (6.2.2)$$

The parameters A and ϕ from equation (6.2.1) are determined with the regression coefficients β_{cos} and β_{sin}: $A = \sqrt{\beta_{cos}^2 + \beta_{sin}^2}$ and $\tan\phi = \beta_{sin}/\beta_{cos}$. [1]

The mean transit time τ_m is then calculated by the damping from in- to output:

$$\tau_m = \frac{\sqrt{f^{-2} - 1}}{c}, \qquad f = \frac{A_{out}}{A_{in}} \text{ (EM)} \qquad (6.2.3)$$

$$\tau_m = \frac{\eta \cdot \sqrt{f^{-2} - 1}}{c} \text{ (EPM)} \qquad (6.2.4)$$

with A_{out} and A_{in}, the amplitudes of in- and output and η, the portion of piston flow: $\eta = 1 \Rightarrow$ EPM = EM, $\eta \to \infty \Rightarrow$ EPM = PM. Values for η have to be assumed and are taken from literature values in this thesis. (Equations (6.2.1) to (6.2.4) cited from McGuire and McDonnell (2006).)

Looking at the isotope time series (e.g. Figure 5.1.1 on page 38) one can see distinct seasonal changes in most of the investigated years. However, these changes show differing amplitudes and are not equally large throughout the years. This is also the case for the respective stream water isotope time series.

To estimate mean transit time in this thesis, the weekly time series of in- and output (2000-2006) have been merged to a "mean year" series, with all samples accumulated and averaged where required (two or more samples on one day). The regression model was applied to the resulting one year time series. For the Zastlerbach catchment, additionally regressions were computed for every year and also over the complete regression period. The results were in agreement with the mean year computations. However, the mean year computations improved the coefficient of determination R^2. Here, no flux-weighting has been done. According to McGuire et al. (2002) this might lead to an over-estimation of mean transit time. Yet, at least the above mentioned maximum value estimation can be seen. Also, the uncorrected precipitation concentrations have been used, but since the mean transit time estimation depends on amplitude damping, and the precipitation concentration amplitude is not varied noteworthy by the height correction, this is considered acceptable.

6.3 Results

In the Zastlerbach catchment sine-wave regressions were computed for the whole time series, yearwise and for the mean year over the investigation period. Because the mean year calculations in the Zastlerbach catchment fit well to

[1] When using the arctan function be aware of the quadrant: if β_{cos} and/or β_{sin} are negative, one or two π have to be added.

Table 6.3.1: Results of the sine-wave regressions, with the mean year "Mean", the respective 21day running average "21day" and period 2000 to 2005 regression values "All".

year	$\beta 0$	β_{cos}	β_{sin}	A	ϕ	days	R^2	adj. R^2
Zastlerbach catchment: precipitation								
Mean	-8.6786	-2.9529	-0.3276	2.9710	3.2521	366	0.419	0.414
21day	-8.6035	-2.8282	-0.3625	2.8513	3.2691	366	0.819	0.818
2005	-7.9261	-1.4524	-0.3052	1.4841	3.3487	365	0.177	0.136
2004	-8.5806	-2.6456	-0.6261	2.7187	3.3740	366	0.426	0.400
2003	-9.1783	-5.0440	-0.5019	5.0689	3.2408	365	0.595	0.574
2002	-9.1980	-2.4104	0.5334	2.4687	2.9238	365	0.251	0.213
2001	-8.5081	-3.1702	-0.7338	3.2540	3.3691	365	0.545	0.525
2000	-8.9891	-3.0614	0.1671	3.0660	3.0871	366	0.357	0.325
All	-8.8208	-2.8959	-0.3729	2.9198	3.2697	365	0.350	0.345
Zastlerbach catchment: runoff								
Mean	-9.8140	0.1561	-0.1222	0.1982	5.6190	366	0.175	0.168
21day	-9.8151	0.1615	-0.1289	0.2066	5.6095	366	0.698	0.696
2005	-9.8500	0.1023	0.0087	0.1027	0.0852	365	0.163	0.127
2004	-9.9053	0.1319	-0.1917	0.2327	5.3151	366	0.160	0.126
2003	-9.8098	0.2544	-0.1972	0.3219	5.6237	365	0.676	0.663
2002	-9.6303	-0.0807	-0.1376	0.1595	4.1821	365	0.252	0.221
2001	-9.9060	0.2578	0.0203	0.2586	0.0786	365	0.204	0.171
2000	-9.8060	0.2868	-0.2282	0.3666	5.6111	366	0.410	0.381
All	-9.8159	0.1471	-0.1113	0.1844	5.6353	365	0.149	0.144
Brugga catchment: precipitation								
Mean	-8.8805	-3.0422	-0.1239	3.0447	3.1823	366	0.505	0.502
21day	-8.8528	-2.9367	-0.1092	2.9388	3.1788	366	0.880	0.879
Brugga catchment: runoff								
Mean	-9.8535	-0.0443	-0.2021	0.2069	4.4968	366	0.182	0.176
21day	-9.8518	-0.0381	-0.2037	0.2072	4.5273	366	0.703	0.701

the results of the single years, only the mean year regression was applied to the Brugga catchment. Also, the diagrams are more compact and comprehensive.

Figure 6.3.1 and 6.3.2 (Zastlerbach) and Figure 6.3.3 and 6.3.4 (Brugga) show the mean year results. The variation of δ^{18}O, illustrated as dots, is already damped for precipitation because the samples are bulk samples. Still, the variability even within days can be seen, but also the superposing seasonal change, which this method applies to. For illustration of this seasonal effect, a 21 day moving average is plotted additionally. The red dashed line is the sine-wave regression finally used. For summarized results see Table 6.3.1. In case of the Zastler catchment, the table also contains the results of single year fits, indicating variations in in- and output over the reflected years. Only in 2002 the regression does not yield reasonable results. All other years show sufficiently sine-shaped variations. Because the mean year regression agreed well to single year regression averages in case of the Zastler catchment, these fits were subsequently omitted in the Brugga catchment. The regression lines which are plotted in the figures show the mean year regressions Nevertheless, the 21day regressions are but hardly different (see 6.3.1).

All diagrams show some outliers that are clearly located outside the "normal" range of variation of about ±2.5 ‰ for the precipitation and about ±0.5 ‰ for the runoff. For the precipitation (Figure 6.3.1 and 6.3.3), where the variability is generally stronger due to different origin and genesis (e.g. convective storm events, cyclonal events with different drift directions and resulting luff-lee effects), no distinct scheme can be seen for explanation of the outlying values except the fact, that the extremely deviating samples are strongly depleted in δ^{18}O and occur in late autumn and winter. That could be caused by weather conditions influenced by strong northern cyclones pumping cold oceanic air masses to central Europe. however, those outliers are rare.

In case of streamwater (Figure 6.3.2 and 6.3.4) a more systematic variability can be seen. During snowmelt in springtime the higher proportion of younger waters cause a wider spreading of streamwater concentrations. This can be observed especially in the Brugga (Figure 6.3.4).

Generally, one can see the phase lag between precipitation and streamwater maximum δ^{18}O concentration. This nearly leads to inversion of the sine-wave function in the Zastler with δ^{18}O precipitation maxima in summer and minima for δ^{18}O in stream water respectively. In the Brugga catchment, the streamwater concentration has its minimum rather in spring than in summer, probably because of the bigger portion of higher elevated areas and subsequently stronger influence of snow runoff effects. The δ^{18}O progression in precipitation looks similar, as the catchments are located side by side.

The streamwater time series indicate, that despite the mountainous character of the catchments with steep slopes and fast runoff reactions, the runoff is composed of older water mobilized by precipitation events, at least in summertime, when precipitation shows distinct higher δ^{18}O concentrations than runoff. This has been studied widely and reported before e.g. by Uhlenbrook et al. (2002).

The sine-wave regressions result in mean transit time estimations of about two to three years, depending on the model type (EM, EPM). As stated above, η had to be assumed in case of the EPM. McGuire and McDonnell (2006) presented a summarizing table with transit time field studies in which an η of about 1.2 for similar scaled catchment was found. EPM results were calculated with this value.

In Table 6.3.2 the respective results are summarized. One can see that the EPM model shows systematic higher results than the EM model. That is not particularly surprising as the piston flow part of the model produces a delay in discharge contribution. More remarkable seems the fact that the Zastlerbach catchment, although smaller than the Brugga, shows longer mean transit times (2.4/2.9 years for EM/EPM) than the Brugga (2.3/2.8) during the investigated period. From a mathematical point of view, this reflects the earlier

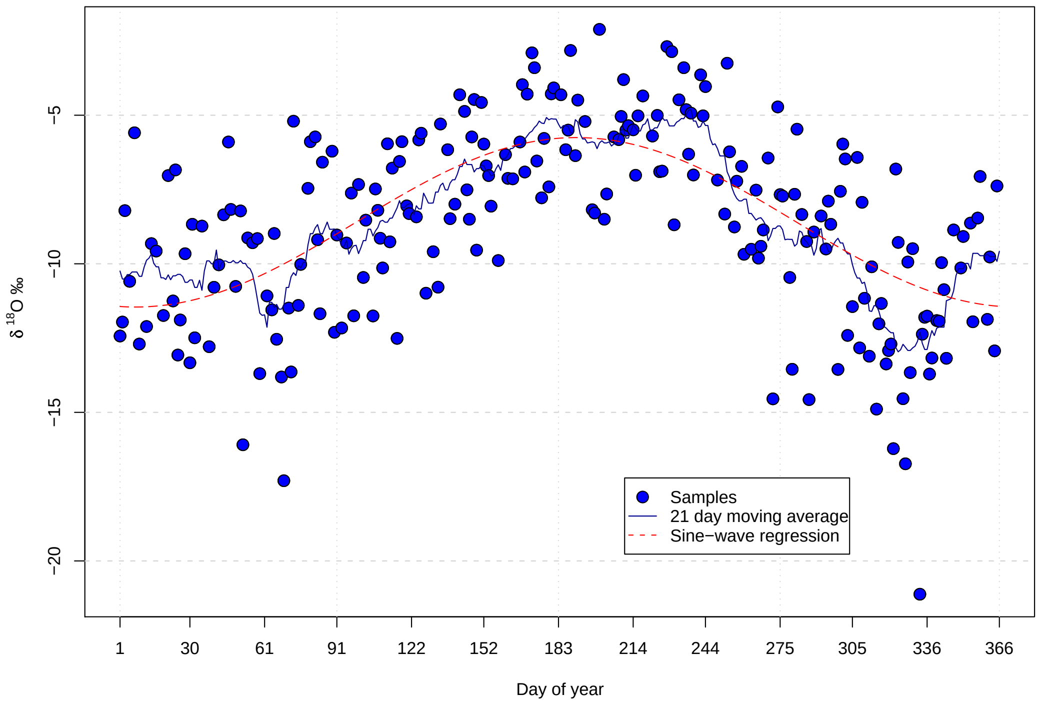

Figure 6.3.1: Zastler catchment, δ^{18}O variation in bulk precipitation samples and fitted sine-wave model, further explanations see text.

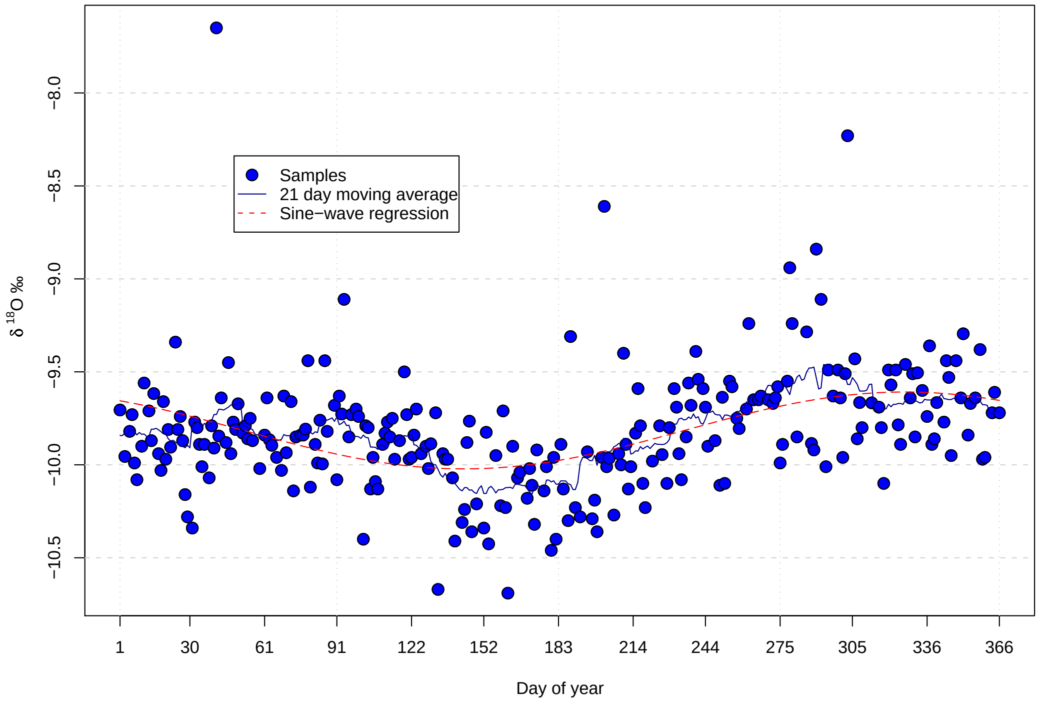

Figure 6.3.2: Zastler catchment, δ^{18}O variation in stream flow samples and fitted sine-wave model, further explanations see text.

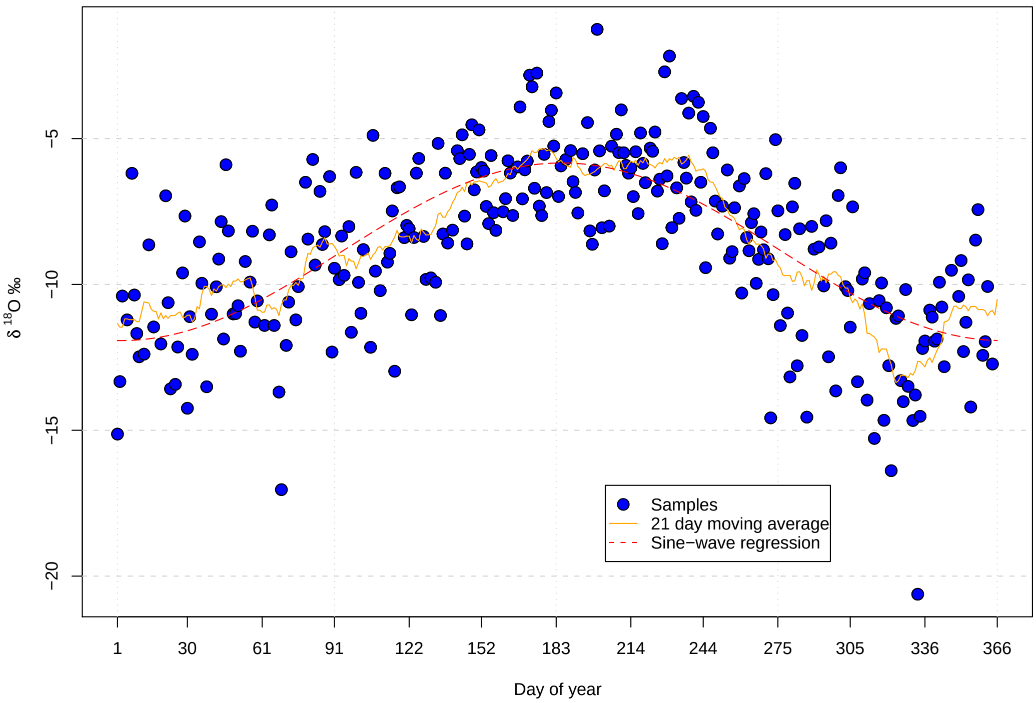

Figure 6.3.3: Brugga catchment, δ^{18}O variation in bulk precipitation samples and fitted sine-wave model, further explanations see text.

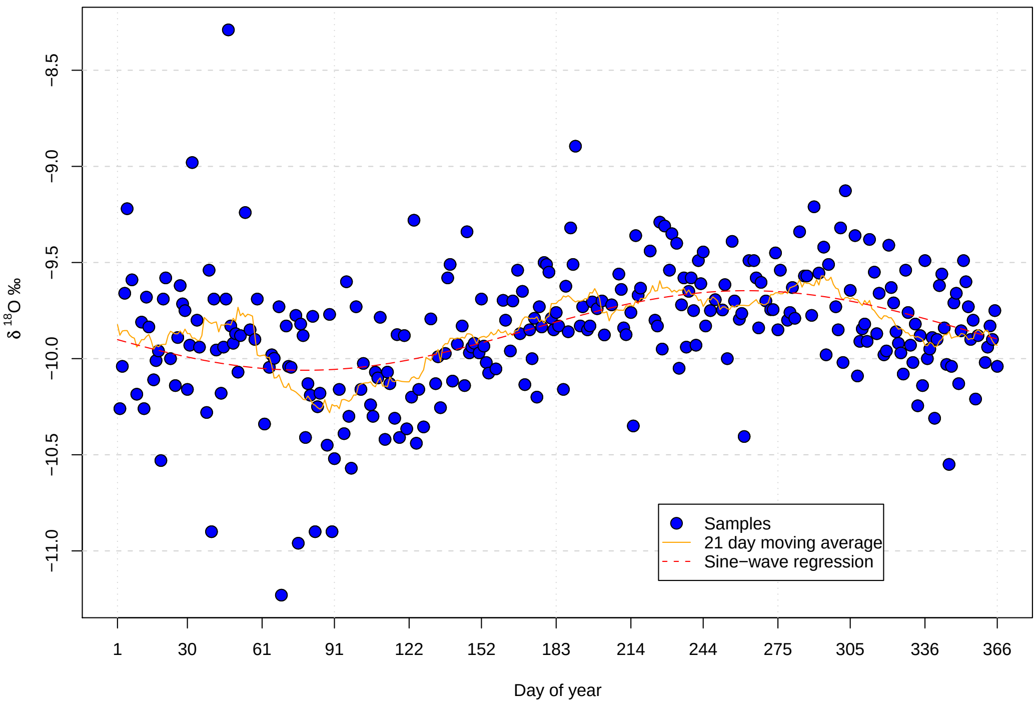

Figure 6.3.4: Brugga catchment, δ^{18}O variation in stream flow samples and fitted sine-wave model, further explanations see text.

Table 6.3.2: EM and EPM model results, $\eta = 1.2$ (see text). With the mean year "Mean", the respective 21day running average "21day" and period 2000 to 2005 results "All".

year	c	f	τ(EM)	τ(EPM)
Zastlerbach catchment				
Mean	0.01717	0.06672	2.4	2.9
21day	0.01717	0.07245	2.2	2.6
2005	0.01721	0.06920	2.3	2.7
2004	0.01717	0.08559	1.8	2.23
2003	0.01721	0.06350	2.5	3.0
2002	0.01721	0.06459	2.4	2.9
2001	0.01721	0.07946	2.0	2.4
2000	0.01717	0.11956	1.3	1.6
All	0.01721	0.06316	2.5	3.0
Brugga catchment				
Mean	0.01717	0.06795	2.3	2.8
21day	0.01717	0.07052	2.3	2.7

δ^{18}O minimum in the Brugga catchment and might be caused hydrologically by the steeper relief in the Brugga catchment or higher snow accumulation (see above).

6.4 Conclusions

The sine wave regression method could be applied to both catchments because both show significant seasonal input variation in δ^{18}O concentration. Regressions resulted in mean transit time estimations of about 2.5 years (Brugga) and about 3 years (Zastlerbach). These values are relatively rough estimations because of the limitations of the regression method but nonetheless provide good maximum estimations and are also comparable to other field study results because the method is widely known and applied.

7 Concluding discussion

7.1 Model applications

Considering the absolute values, the sine-wave regression yielded substancially longer mean transit times than the conceptual approach. Depending on the distribution model mean transit times of 2.5 to 3 years were computed. The conceptual approach results in mean transit times of 1 to 1.4 years. As cited in the sine-wave chapter, this was also experienced in other studies.

But, the main benefit of the conceptual transit time model is certainly not an improved estimation of mean transit times over longterm periods, but more the possibility to assess the development during hydrological interesting phases like extreme situations. I.e., the modelled results illustrate that event water can contribute noteworthy to the runoff reaction but does not distinctly alterate the isotopic concentration in runoff.

7.2 Limitations and issues

A conceptual approach bears always the risk that important processes have not been understood correctly and thus are implemented wrongly or even neglected completely in a model scheme. Additionally, the higher the parametrisation of a conceptual model, the higher is also the risk that model deficiencies are covered by the plenty of degrees of freedom being available for the response function.

In the case of this thesis a, for its purpose well working, precipitation-runoff model was modified in order to fit the requirements of a transport model. The structure of the HBV model, e.g. the dead end soil storage with the FC parameter, comprises several trade-offs between a functional reproduction of catchment behaviour and actual catchment processes and is certainly not likely to depict catchment reality above a certain degree. If this structure is adopted to model a different process like the transit time development, it is probably appropriate to be cautious with the results.

7.3 Final remarks

The results of the applied methods are in principle pleasant. The hypothesis of mean transit time overestimation by the sine-wave method proved true and the simulated transit time development in connection with the dry summer 2003 makes sense from a hydrological point of view.

Nevertheless, it is difficult to determine the validity of the model results. A validation with additional data, e.g. aquifer $\delta^{18}O$ sampling, would give the possiblity to consolitate (or discard, of course) the modelled results.

A Appendix

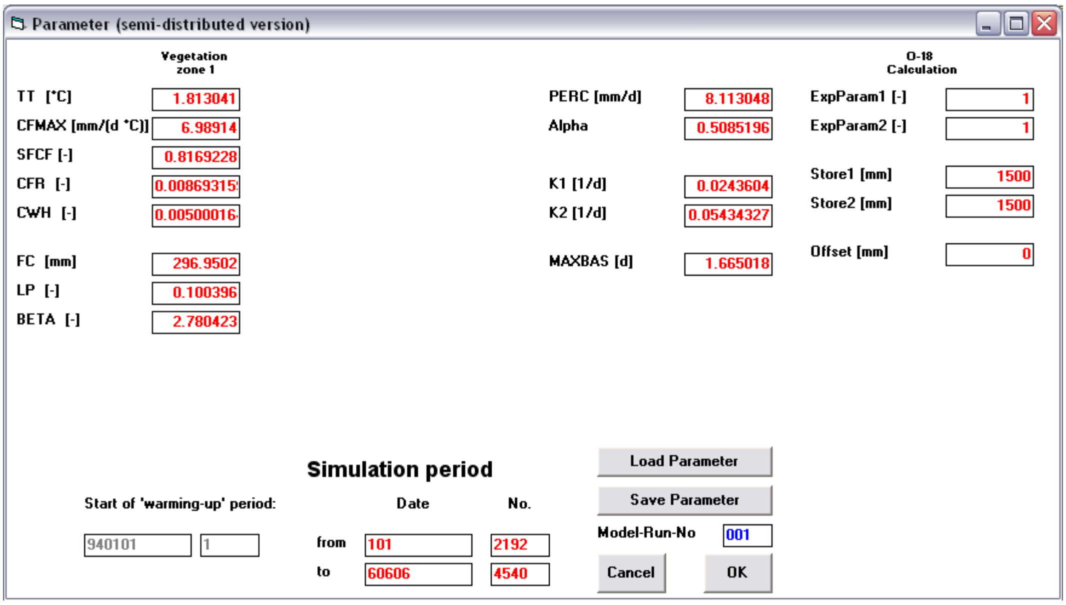

Figure A.1: The HBV - ^{18}O parameter interface.

Table A.1: Parameter sets used for the simulations in both catchments.

	Zastlerbach catchment	Brugga catchment		
	Veg. Zone 1	Veg. Zone 1	Veg. Zone 2	Veg. Zone 3
TT	1.813041	2.716867	0.2633334	-1.999433
CFMAX	6.98914	5.49995	4.229291	5.47408
SFCF	0.8169228	0.8951042	1.413672	0.6730116
CFR	0.008693159	0.01000075	0.02758498	0.04580348
CWH	0.005000164	0.1299922	0.1159813	0.06413436
FC	296.9502	249.9915	249.9992	249.9585
LP	0.100396	0.6000021	0.6000291	0.6001931
BETA	2.780423	2.999982	2.184225	2.749167
PERC	8.113048	5.674984	–	–
UZL	0.5085196	0.2810796	–	–
K0	0	0	–	–
K1	0.0243604	0.05558046	–	–
K2	0.05434327	0.05920349	–	–
MAXBAS	1.665018	1.435005	–	–
CET	0	0	–	–

Table A.2: Elevation and vegetation zoning for both catchments.

	Zastlerbach catchment	Brugga catchment		
Elev. Zone	Veg. Zone 1	Veg. Zone 1	Veg. Zone 2	Veg. Zone 3
450	-	0.009	0.001	0.008
550	0.0076	0.031	0.02	0.002
650	0.0531	0.018	0.048	0
750	0.0674	0.007	0.062	0.007
850	0.0885	0.019	0.081	0.002
950	0.1172	0.02	0.119	0.001
1050	0.2014	0.052	0.159	0.002
1150	0.2607	0.058	0.139	0
1250	0.139	0.029	0.074	0
1350	0.0393	0.019	0.009	0
1450	0.0258	0.004	0	0

Bibliography

S. Bergström. Principles and confidence in hydrological modelling. *Nordic Hydrology*, 22:123–136, 1991.

S. Bergström. *Computer Models of Watershed Hydrology*, chapter 13. Water Resources Publications, 1995. ISBN 0-918334-91-8.

K. J. Beven. *Rainfall-runoff modelling : the primer*. John Wiley & Sons, 1st edition, 2001. ISBN 0-471-98553-8.

C. I. Bliss. *Periodic Regression Statistics in Biology*, pages 219–287. McGraw-Hill Book Co., New York, 1970.

R. Courant and H. Robbins. *Was ist Mathematik?* Springer, 2000. ISBN 3-540-63777-X.

D. R. DeWalle, P. J. Edwards, B. R. Swistock, R. Aravena, and R. J. Drimmie. Seasonal isotope hydrology of three appalachian forest catchments. *Hydrological Processes*, 11:1895–1906, 1997.

J. Didszun. *Abflussbildung an Hängen*. Diplomarbeit, Albert-Ludwigs-Universität Freiburg i. Br., Institut für Hydrologie, 2000.

DVWK. *Ermittlung der Verdunstung von Land- und Wasserflächen*. Number 238 in DVWK-Merkblätter zur Wasserwirtschaft. Deutscher Verband für Wasserwirtschaft und Kulturbau e.V. - Wirtschafts- und Verl.-Ges. Gas und Wasser, Bonn, 1996. ISBN 3-89554-034-X.

S. Dyck and G. Peschke. *Grundlagen der Hydrologie*. Verl. für Bauwesen, Berlin, 3rd edition, 1995. ISBN 3-345-00586-7.

T. Ehnes. *Der Einfluss der Schneeschmelze auf die Abflussbildung und die Grundwasserneubildung im Einzugsgebiet der Dreisam*. Diplomarbeit, Albert-Ludwigs-Universität Freiburg i. Br., Institut für Hydrologie, 2006.

J. R. Gat. Oxygen and hydrogen isotopes in the hydrologic cycle. *Annu. Rev. Earth Planet. Sci.*, 24:225–262, 1996.

M. Holocher. *Anwendung des Niederschlags-Abfluss-Modells HBV an der Dreisam und verschieden skalierten Teileinzugsgebieten*. Diplomarbeit, Albert-Ludwigs-Universität Freiburg i. Br., Institut für Hydrologie, 1997.

R. Holzschuh. *Planung und Einrichtung eines Messnetzes zur Erfassung der regionalen Isotopenverteilung im Niederschlag.* Diplomarbeit, Albert-Ludwigs-Universität Freiburg i. Br., Institut für Hydrologie, 1995.

C. Kendall and J. J. McDonnell, editors. *Isotope tracers in catchment hydrology.* Elsevier, Amsterdam, 1st edition, 1998. ISBN 0-444-81546-5.

LfU. Landesamt für umweltschutz: Pegelstatistik und hydrologische hauptzahlen der pegel brugga, dreisam, st. wilhelmer talbach, zastlerbach und wagensteigbach. unpublished, 2000.

M. Lindenlaub. *Abflußkomponenten und Herkunfträume im Einzugsgebiet der Brugga : Aspekte zeitlicher und räumlicher Skalierung.* Diplomarbeit, Albert-Ludwigs-Universität Freiburg i. Br., Institut für Hydrologie, 1998.

G. Lindström and A. Rodhe. Modelling water exchange and transit times in till basins using oxygen-18. *Nordic Hydrology*, 17:325–334, 1986.

P. Maloszewski and A. Zuber. Determining the turnover time of groundwater systems with the aid of environmental tracers. *Journal of Hydrology*, 57: 207–231, 1982.

K. J. McGuire and J. J. McDonnell. A review and evaluation of catchment transit time modeling. *Journal of Hydrology*, 2006. article in press.

K. J. McGuire, D. R. DeWalle, and W. J. Gburek. Evaluation of mean residence time in subsurface waters using oxygen-18 fluctuations during drought conditions in the mid-appalachians. *Journal of Hydrology*, 261:132–149, 2002.

H. Moser and W. Rauert, editors. *Isotopenmethoden in der Hydrologie.* Number 8 in Lehrbuch der Hydrogeologie. Gebrüder Bornträger, Berlin - Stuttgart, 1980. ISBN 3-443-01012-1.

P. Rodgers, C. Soulsby, S. Waldron, and D. Tetzlaff. Using stable isotope tracers to assess hydrological flow paths, residence times and landscape influences in a nested mesoscale catchment. *Hydrology and Earth System Sciences*, 9:139–155, 2005.

J. Seibert. Hbv light version 2 user's manual. unpublished, 2002.

J. Seibert, A. Rodhe, and K. Bishop. Simulating interactions between saturated and unsaturated storage in a conceptual runoff model. *Hydrological Processes*, 17:379–390, 2003.

C. Soulsby, R. Malcolm, R. Helliwell, R. C. Ferrier, and A. Jenkins. Isotope hydrology of the allt a' mharcaidh catchment, cairngorms, scotland: implications for hydrological pathways and residence times. *Hydrological Processes*, 14:747–762, 2000.

I. Stober. *Die Wasserführung des kristallinen Grundgebirges : 16 Tabellen.* Enke, Stuttgart, 1st edition, 1995. ISBN 3-432-26771-1.

H. Trenkle and H. v. Rudolf. Das klima im schwarzwald. In E. Liehl and W. D. Sick, editors, *Der Schwarzwald - Beiträge zur Landeskunde*, pages 59–100. Konkordia, Bühl/Baden, 1989. ISBN 3-7826-0047-9.

S. Uhlenbrook. *Untersuchung und Modellierung der Abflussbildung in einem mesoskaligen Einzugsgebiet.* Number 10 in Freiburger Hydrologische Schriften. Institut für Hydrologie der Universität Freiburg, 1999a.

S. Uhlenbrook, J. Seibert, C. Leibundgut, and A. Rodhe. Prediction uncertainty of conceptual rainfall-runoff models caused by problems in identifying model parameters and structure. *Hydrological Sciences Journal*, 44(5):779–797, 1999b.

S. Uhlenbrook, M. Frey, C. Leibundgut, and P. Maloszewski. Hydrograph separations in a mesoscale mountainous basin at event and seasonal timescales. *Water Resources Research*, 38(6), 2002.

URL1. http://www.r-project.org/.

L. Wissmeier. *Implementation of distributed solute transport into the catchment model* TAC^d *and event based simulations using oxygen-18.* Diplomarbeit, Albert-Ludwigs-Universität Freiburg i. Br., Institut für Hydrologie, 2005.

Ehrenwörtliche Erklärung:

Hiermit erkläre ich, dass die Arbeit selbständig und nur unter Verwendung der angegebenen Hilfsmittel angefertigt wurde.

Ort, Datum

Unterschrift